Materials Science & Engineering A 850 (2022) 143586

Contents lists available at ScienceDirect

Materials Science & Engineering A

journal homepage: www.elsevier.com/locate/msea

Critical resolved shear stress for twinning and twinning-induced plasticity in single crystals of the $CoCrFeNiMo_{0.2}$ high-entropy alloy

I.V. Kireeva *, Yu.I. Chumlyakov, A.V. Vyrodova, A.A. Saraeva

National Research Tomsk State University, Siberian Physical-Technical Institute of V.D. Kuznetsova, Novosobornaya Sq.1, Tomsk, 634050, Russia

ARTICLE INFO

Keywords:
$CoCrFeNiMo_{0.2}$ high-entropy alloy
Single crystals
Tensile strain
Deformation twinning
Twinning-induced plasticity

ABSTRACT

The effect of alloying with Mo atoms 4 at.% on the twinning deformation, critical resolved shear stresses (CRSS) for slip τ_{cr}^{sl} and twinning τ_{cr}^{tw} and plasticity was studied in $[\bar{1}11]$-, $[\bar{1}44]$- and [001]- oriented crystals of the $Co_{24}Cr_{24}Fe_{24}Ni_{24}Mo_4$ (at.%) high-entropy alloy (HEA) under tension at 296 and 77 K. The stacking fault energy of the $Co_{24}Cr_{24}Fe_{24}Ni_{24}Mo_4$ HEA, measured in the present paper on the triple dislocation nodes, is equal to 0.027 J/m^2. It is shown that initial yield behavior along studied orientations is governed by dislocation slip and the CRSS for slip are independent of crystal orientation. Under tensile strain, twinning develops in the $[\bar{1}11]$- and $[\bar{1}44]$- oriented crystals only at 77 K and is not detected in the [001]-oriented crystals. Two types of twins are found in the $[\bar{1}11]$- and $[\bar{1}44]$-oriented crystals (thin nanotwins and macrotwins). Nanotwins develop after a low slip deformation of 5–10% and are observed only by transmission electron microscopy. Macrotwins are detected after a significant slip deformation of 20 and 60% and are determined metallographically and X-ray by the precession of the crystal axis, respectively, in the $[\bar{1}11]$- and $[\bar{1}44]$-oriented crystals. In the $[\bar{1}11]$- oriented crystals, there is no precession of the crystal axis due to the development of slip simultaneously in several systems. It is shown that CRSS for nano- and macrotwins are dependent on the crystal orientation. In the $[\bar{1}44]$-oriented crystals, $\tau_{cr}^{tw} = 212$ MPa for nanotwinning and $\tau_{cr}^{tw} = 400$ MPa for macrotwinning. In the $[\bar{1}11]$-oriented crystals, $\tau_{cr}^{tw} = 250$ MPa for nanotwinning and $\tau_{cr}^{tw} = 335$ MPa for macrotwinning. For the transition to deformation by macrotwinning, it is necessary that the effective stacking fault energy γ_{ef} is approaching to zero and the condition $\tau_{cr}^{tw} < \tau_{cr}^{sl}$ is satisfied. Deformation by macrotwinning suppresses slip multiplicity and shifts the formation of the neck formation according to the Considère condition to higher stress levels. This increases plasticity from 72% at 296 K to 108% at 77 K in $[\bar{1}44]$-oriented crystals and from 48% at 296 K to 57% at 77 K in $[\bar{1}11]$-oriented crystals.

1. Introduction

High entropy alloys (HEAs) are a new class of materials that do not have a "base element" and are a mixture of five or more principal elements, whose concentrations vary from 5 to 35 at.% [1–5]. Detailed features of the HEA structure were considered in the reviews [2,5]. Stable HEAs with face-centred cubic (fcc) lattice have a high strain hardening, good plasticity and ductile fracture, especially at the cryogenic temperature range [3,4,6–11]. Due to the high plasticity associated with twinning, the fcc HEAs can be considered as TWIP alloys (TWIP is twinning induced plasticity) [12]. However, fcc HEAs are not strong enough for practical applications [1,4–9]. Therefore, the stress level at the yield point in the fcc HEAs was increased in various ways without loss of plasticity due to: i) alloying with substitution atoms with a large atomic radius compared to the atoms that form the basis of the system, for instance, atoms of Al, Ti, Mo [8,13–17]; ii) solid solution hardening by the interstitial atoms (nitrogen and carbon) [18]; iii) precipitation hardening [13,16,19–22]; iv) reducing the grain size [6]; v) cold deformation [23–25] and so on.

It is well known that in fcc pure metals and their substitutional and interstitial alloys, the development of twinning is determined by several factors: the stacking fault energy γ_0, the level of deforming stresses at the yield point $\sigma_{0.1}$, the test temperature, the crystal orientation, the texture and grain size in polycrystals, method of deformation (tension and compression) [12,26–36]. Twinning deformation in fcc pure metals and their substitutional and interstitial alloys was always preceded by slip, due to which the required stress level for twinning was achieved [26–28,31,32,34]. Despite numerous publications, twinning deformation in

* Corresponding author.
E-mail address: kireeva@spti.tsu.ru (I.V. Kireeva).

https://doi.org/10.1016/j.msea.2022.143586
Received 11 May 2022; Received in revised form 8 July 2022; Accepted 10 July 2022
Available online 13 July 2022

single- and polycrystals of fcc HEAs has not been fully understood. There are no systematic studies in the literature on the effect of solid-solution hardening by substitution atoms of a larger atomic radius than system atoms on the transition from slip to macrotwinning, on the level of critical resolved shear stresses (CRSS) for twinning τ_{cr}^{tw}, the τ_{cr}^{tw} dependence on the γ_0 value, test temperature and crystal orientation or texture in polycrystals. The data available in the literature for $\tau_{cr}^{tw} = 235$ MPa were obtained under tensile strain untextured polycrystals of the equiatomic CoCrFeMnNi HEA with a grain size of d = 17 μm at 296 and 77 K [37]. In this case, nanotwins were detected in the study of the dislocation structure using transmission electron microscopy (TEM). The $\tau_{cr}^{tw} = 154$ MPa was obtained for $[\bar{1}44]$-oriented crystals of the equiatomic CoCrFeMnNi HEA under tension at 77 K using of the digital image correlation (DIC) [29,30]. The use of TEM and X-ray in the study of twinning in the equiatomic CoCrFeMnNi HEA single crystals made it possible to detect a difference in the τ_{cr}^{tw} values for the appearance of nanotwins under tension by the TEM method and macrotwinning using X-ray, when studying the precession of crystal axis at 296 and 77 K [9]. The stresses for τ_{cr}^{tw} obtained using X-ray were significantly higher than those for τ_{cr}^{tw} found using TEM [9]. However, there was no unambiguous answer to the definition of τ_{cr}^{tw} for fcc HEAs, as well as data on the relationship between twinning and the value of preliminary slip deformation before twinning and plasticity. This requires additional studies on HEA single crystals.

In fcc HEAs with stacking fault energy $\gamma_0 = 0.02–0.05$ J/m^2, twinning plays a decisive role in achieving high plasticity at cryogenic temperatures [3,6–9,20,29–33]. The lower was the stacking fault energy γ_0, the lower were the stresses for the nucleation of twins [8,9]. The peculiarity of the fcc HEAs in relation to the development of twinning is determined by the following points. Firstly, the structure of the fcc HEA solid solution suppresses the growth of large twins, and the stage of nucleation and growth of twins is extended along the stress-strain ($\sigma(\varepsilon)$) curve in a wide stress range. As a result, there is no sharp transition from slip to twinning in fcc HEAs, and twinning always develops simultaneously with slip, as in single- and polycrystals of Hadfield steel and austenitic stainless steels [6–9,19,20,29–34,38]. Secondly, with a decrease in the test temperature, the level of deforming stresses in the fcc HEAs increases due to the strong temperature dependence of the yield point $\sigma_{0.1}(T)$. In this case, the slip deformation reduces to twinning, and twinning is shifted to the beginning of plastic flow [6–9,31–33,37]. For instance, at 77 K in the $[\bar{1}44]$-oriented CoCrFeMnNi HEA crystals, when the slip deformation was practically suppressed, twinning developed simultaneously in several systems after strain of 10% [9]. In this case, there was a sharp increase in the strain hardening coefficient $\Theta = d\sigma/d\varepsilon$ and a decrease in plasticity by a factor of two compared to room temperature, when twinning developed in one system after a significant slip deformation of 50% (at 296 K, the plasticity was equal to 110%, and at 77 K it decreased up to 50%). At 77 K, in the $[\bar{1}44]$-oriented CoCrFeMnNi HEA crystals with the development of only twinning deformation, the failure occurred via a quasi-cleavage process, which is not typical for fcc HEAs [9]. Thirdly, fcc HEAs are concentrated solid solutions. In such solutions, the role of short-range order (SRO) increases, which counteracts the movement of dislocations, including twinning ones [8,39–41]. In the case of slip deformation, SRO promotes the localization of deformation in one system and the development of a planar dislocation structure with pile-ups [8,41–43]. With regard to twinning deformation, the SRO blocks the formation of large twins due to the need for its destruction by twinning dislocations in each {111} plane, increases τ_{cr}^{tw} for twinning and can even completely suppress twinning [8,9,44,45].

In present paper, we studied the effect of alloying with Mo atoms 4 at.% on the development of twinning, CRSS for slip τ_{cr}^{sl} and twinning τ_{cr}^{tw} and plasticity in single crystals of the equiatomic CoCrFrNi (at.%) HEA. Alloying with Mo atoms up to 4 at.% was carried out by reducing the concentration of each element of the CoCrFeNi system in equal atomic percentages. Thus, $Co_{24}Cr_{24}Fe_{24}Ni_{24}Mo_4$ (at.%) HEA was obtained, which had a mixing entropy of 12.5 J/mol·K. The choice of Mo atoms with a concentration of 4 at.% for alloying the CoCrFeNi system was due to the following circumstances. Firstly, alloying with Mo increases the corrosion resistance of HEAs, which is important for practical applications [17,46]. Secondly, the Mo atoms have an atomic radius larger than the atoms of the CoCrFeNi system, and this leads to solid solution strengthening. Indeed, when alloyed with Mo atoms with a concentration of 6 at.% of as-cast CoCrFeNi alloy at 296 K, the yield point $\sigma_{0.1}$ increased from 155 MPa to 305.3 MPa. Assuming the Taylor factor of 3.06, the CRSS for slip τ_{cr}^{sl} increased from 50 MPa to 99.7 MPa, respectively [17]. However, the solubility of Mo atoms in the HEA solid solution is limited. In the HEA solid solution, Mo can be present up to concentrations of 6 at.%. At higher Mo concentrations, precipitation of intermetallic σ- and μ-phases occurs during quenching [17]. Intermetallic σ- and μ-phases also precipitate during ageing at temperatures of 1073–1173 K and provide particle hardening of fcc HEAs with Mo [17,22,47]. Thirdly, alloying with Mo reduces the γ_0 value and promotes the development of twinning [17,48]. Thus, in the equiatomic CoCrFeNi HEA, the γ_0 value was 0.030 J/m^2 [3,17]. When alloyed with Mo at concentration of 4.6 at.%, γ_0 decreased to 0.019 J/m^2 in as-extruded $CoCrFeNiMo_{0.23}$ HEA [48]. A decrease in γ_0 in as-extruded $CoCrFeNiMo_{0.23}$ HEA caused the formation of stacking faults (SFs) and twins at 296 K, which were not found in the annealed $CoCrFeNiMo_{0.23}$ HEA, and led to an increase in strength and plasticity [48].

Experiments using single crystals to study twinning in fcc HEAs provide a number of advantages over polycrystals: i) eliminate the influence of grain boundaries and their different orientation with respect to external stresses on the deformation mechanisms (slip and twinning); ii) allow to control the number of active slip and twinning systems and to investigate their influence on plasticity, due to the choice of orientation; iii) make it possible to investigate the dependence of τ_{cr}^{sl} and τ_{cr}^{tw} on the crystal orientation, the test temperature, the method of deformation (tension and compression) and the value of γ_0; and iv) determine the deformation mechanism (slip or twinning) using TEM and X-ray method of precession of the crystal axis, [8,9,12,20,21,29–33]. In the present paper, and $[\bar{1}44]$ orientations were chosen for the study as the most favorable for the development of twinning by the nucleation and growth of intrinsic SFs under tension in fcc crystals in several and one system, respectively [29,30]. In these orientations under tension, the Schmid factor for twinning m_{tw} is greater than the Schmid factor for slip m_{sl} ($m_{tw} = 0.31$ and $m_{sl} = 0.27$ in $[\bar{1}11]$-oriented crystals and $m_{tw} = 0.5$ and $m_{sl} = 0.4$ in $[\bar{1}44]$-oriented crystals) [30]. As for the [001] orientation under tension, twinning by the mechanism of nucleation and growth of intrinsic SFs is prohibited, since $m_{tw} = 0.24$ is smaller than $m_{sl} = 0.41$ [26,29,30]. Nevertheless, in [001]-oriented crystals under tensile strain, twinning can develop by the mechanism of nucleation and growth of extrinsic SFs, for which $m_{tw} = 0.47$ [33]. Twinning by the mechanism of nucleation and growth of extrinsic SFs was previously observed in [001]-oriented crystals of the equiatomic CoCrFeMnNi HEA under tensile strain at 77 K [33].

Thus, the main goal of paper is to study the develop $[\bar{1}11]$ ment of twinning, to determine the CRSS for slip τ_{cr}^{sl} and for twinning τ_{cr}^{tw} and the effect of twinning on plasticity of $Co_{24}Cr_{24}Fe_{24}Ni_{24}Mo_4$ HEA single crystals, oriented along the $[\bar{1}11]$, $[\bar{1}44]$ and [001] directions under tensile strain.

2. Experimental methods

Single crystals of the $Co_{24}Cr_{24}Fe_{24}Ni_{24}Mo_4$ (at.%) ($CoCrFeNiMo_{0.2}$) HEA were grown by the Bridgman method in alumina (Al_2O_3) crucibles and helium atmosphere, using ingots cast in a resistance furnace. To achieve a homogeneous distribution of the elements in the bulk of the ingots, they were remelted three times. The crucibles had a conical shape with a diameter of 38 mm and a length of 100 mm. To determine

the crystal orientation and the variation of orientation (precession) during deformation, the diffractometric method was used by means of a DRON-3M X-ray diffractometer with monochromatic Fe Kα radiation, the technique of which was presented in Ref. [49]. Determined orientations are shown in Fig. 1. Dog-bone-shaped tension samples with a gauge length of 12 mm and a cross section of 2×1.5 mm^2 were cut using wire electrical discharge machining. The damaged surface layer was ground off mechanically, and then electrically polished in 200 ml of an H_3PO_4 + 50 g CrO_3 (phosphoric acid with chromium trioxide) electrolyte at room temperature. The crystals were homogenized in a helium atmosphere at 1473 K for 48 h and then quenched into water. The chemical composition of the single crystals after quenching was determined using the X-ray fluorescence method, by means of a wavelength dispersive X-ray fluorescence XRF-1800 spectrometer, giving the atomistic percentages Co = 23.65%, Cr = 24.64%, Fe = 23.47%, Ni = 23.58% and Mo = 4.65 (at.%). To determine the alloying elements (Co, Cr, Fe, Ni, Mo), as well as their distribute over the sample, a scanning electron microscope (SEM) TESCAN VEGA3 with an energy dispersive spectroscopy (EDS) detector was used. SEM-EDS maps revealed homogenously distribution of all elements in the area of study (250×250 μm^2), taken in different places of the sample surface, suggesting a single-phase solid solution of single crystals after quenching (Fig. 2). SEM-EDS maps were made on 10 for each orientation. TEM studies were performed in a JEOL-2010 electron microscope at an accelerating voltage of 200 kV. The thin foils were prepared using double-jet electropolishing (TenuPol-5) with an electrolyte containing 20% sulphuric acid in methyl alcohol at room temperature, with 12.5 V applied voltage. The surfaces of deformed samples were examined in a KEYENCE VHX-2000 optical microscope. Mechanical tests were carried out in an Instron 5969 universal testing machine at a strain rate of 4×10^{-4} s^{-1}. Tests at room temperature were carried out in air. For test at 77 K, the sample and grips were immersed in a special vessel with liquid nitrogen, in which both were held for 10 min before the start of the test and then the sample was deformed in liquid nitrogen until failure. The true strain was calculated based on the data obtained from an extensometer directly attached to the gauge section of samples. True stress was calculated considering the variation in cross-section area based on the assumption of a constant volume of the specimen. The CRSS for slip were calculated using an expression $\tau_{cr}^{sl} = \sigma_{0.1} * m_{sl}$ (where $\sigma_{0.1}$ is the uniaxial stress at the 0.1% offset strain yield point). The CRSS for nano- and macrotwinning were calculated using the equation $\tau_{cr}^{tw} = \sigma_{\varepsilon} * m_{tw}$ (where σ_{ε} is the stress corresponding to the minimum strain level at which twinning is revealed by TEM and X-ray diffraction, respectively, for nano- and macrotwinning) [50,51]. X-ray analysis and TEM showed that the single crystals had the expected fcc structure after quenching.

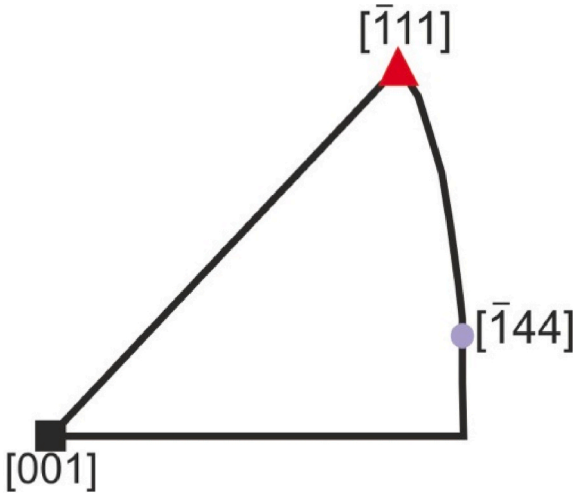

Fig. 1. Orientations of single crystals studied under tension in the present paper.

3. Experimental results

3.1. Critical resolved shear stress for slip

The CRSS for slip τ_{cr}^{sl} for CoCrFeNiMo$_{0.2}$ HEA single crystals under tensile strain at two test temperatures of 296 and 77 K are presented in Table 1. For comparison, τ_{cr}^{sl} for single crystals of the equiatomic CoCrFeMnNi and CoCrFeNiAl$_{0.3}$ HEAs are also presented in Table 1. Analysis of the presented data shows, firstly, that in the CoCrFeNiMo$_{0.2}$ HEA single crystals, as in two other HEA single crystals, τ_{cr}^{sl} do not depend on the crystal orientation. Therefore, the Schmid law is fulfilled. Secondly, alloying with Mo atoms, as well as with Al atoms, leads to solid solution hardening due to a larger atomic radius than that of atoms of the equiatomic CoCrFeMnNi HEA. As a result, τ_{cr}^{sl} in CoCrFeNiMo$_{0.2}$ HEA single crystals turned out to be larger than in equiatomic CoCrFeMnNi HEA single crystals [9].

3.2. Tensile behaviour of [$\bar{1}$11]-oriented single crystals

Fig. 3 displays the σ(ε) curves and the variation in the strain hardening coefficient $\Theta = d\sigma/d\varepsilon$ with tensile strain at 77 and 296 K of the CoCrFeNiMo$_{0.2}$ HEA single crystals oriented along the [$\bar{1}$11] direction. It can be seen that in the [$\bar{1}$11]-oriented crystals, the plastic flow begins from stage II of linear hardening at both test temperatures (Fig. 3a), as in fcc pure metals and substitutional alloys oriented for multiple shear for slip deformation [50,51]. However, the change in Θ with an increase in the strain level depends on the test temperature (Fig. 3b).

At 296 K, after the yield point $\sigma_{0.1}$, an increase in Θ = 1950 MPa is observed with an increase in strain up to 32%, which is characteristic of the slip-slip interaction in fcc crystals [50,51]. Studies of the dislocation structure and optical metallography show that the deformation at this stage develops by slip (Fig. 4a and b). In [$\bar{1}$11]-oriented crystals of the equiatomic CoCrFeMnNi HEA with γ_0 = 0.019–0.021 J/m^2 [3,6,52], twinning was observed in one system at a strain of 5% at 296 K, which developed simultaneously with slip [9,53]. To elucidate the reason for the absence of twinning at low strain levels in CoCrFeNiMo$_{0.2}$ HEA single crystals, the γ_0 value was determined from triple dislocation nodes at 296 K in two HEAs, namely, CoCrFeNi and CoCrFeNiMo$_{0.2}$ HEA single crystals. The γ_0 value is 0.031 J/m^2 in CoCrFeNi HEA single crystals and 0.027 J/m^2 in CoCrFeNiMo$_{0.2}$ HEA. These γ_0 values are in good agreement with γ_0 previously obtained for the fcc HEAs in Refs. [3,17]. Alloying with Mo atoms 4 at.% slightly lowered γ_0, and the γ_0 value in CoCrFeNiMo$_{0.2}$ HEA was greater than in the equiatomic CoCrFeMnNi HEA [3,6,52]. This explains the difference in the development of twinning in [$\bar{1}$11]-oriented crystals of the CoCrFeNiMo$_{0.2}$ and CoCrFeMnNi HEAs at room test temperature. Therefore, in the [$\bar{1}$11]-oriented CoCrFeNiMo$_{0.2}$ HEA crystals at 296 K, slip is the main mechanism of deformation that determines hardening at the linear stage, as was previously established for low-strength fcc metals and their substitutional alloys and [$\bar{1}$11]-oriented crystals of another CoCrFeNiAl$_{0.3}$ HEA [8,50,51]. After the completion of the linear stage, a decrease in Θ is observed (Fig. 3b) and a transition to stage III of the dynamic recovery occurs [50,51]. Plasticity reaches 45% at 296 K.

At 77 K, the Θ(ε) dependence with increasing strain cardinally differs from the observed Θ(ε) dependence at 296 K. Thus, the Θ(ε) dependence initially exhibits a drop in Θ up to 8%. At ε>8%, Θ increases from 1620 MPa to 1900 MPa at 30% strain. Then Θ remains unchanged up to 45% and decreases again at ε>45% (Fig. 3b). Such behavior of Θ with an increase in strain level is characteristic of the development of twinning simultaneously with slip, and it was previously observed in single and polycrystals of the equiatomic CoCrFeMnNi HEA, single crystals of Fe40Mn40Cr10Co10 HEA at 296 K and polycrystals of CrFeNi and

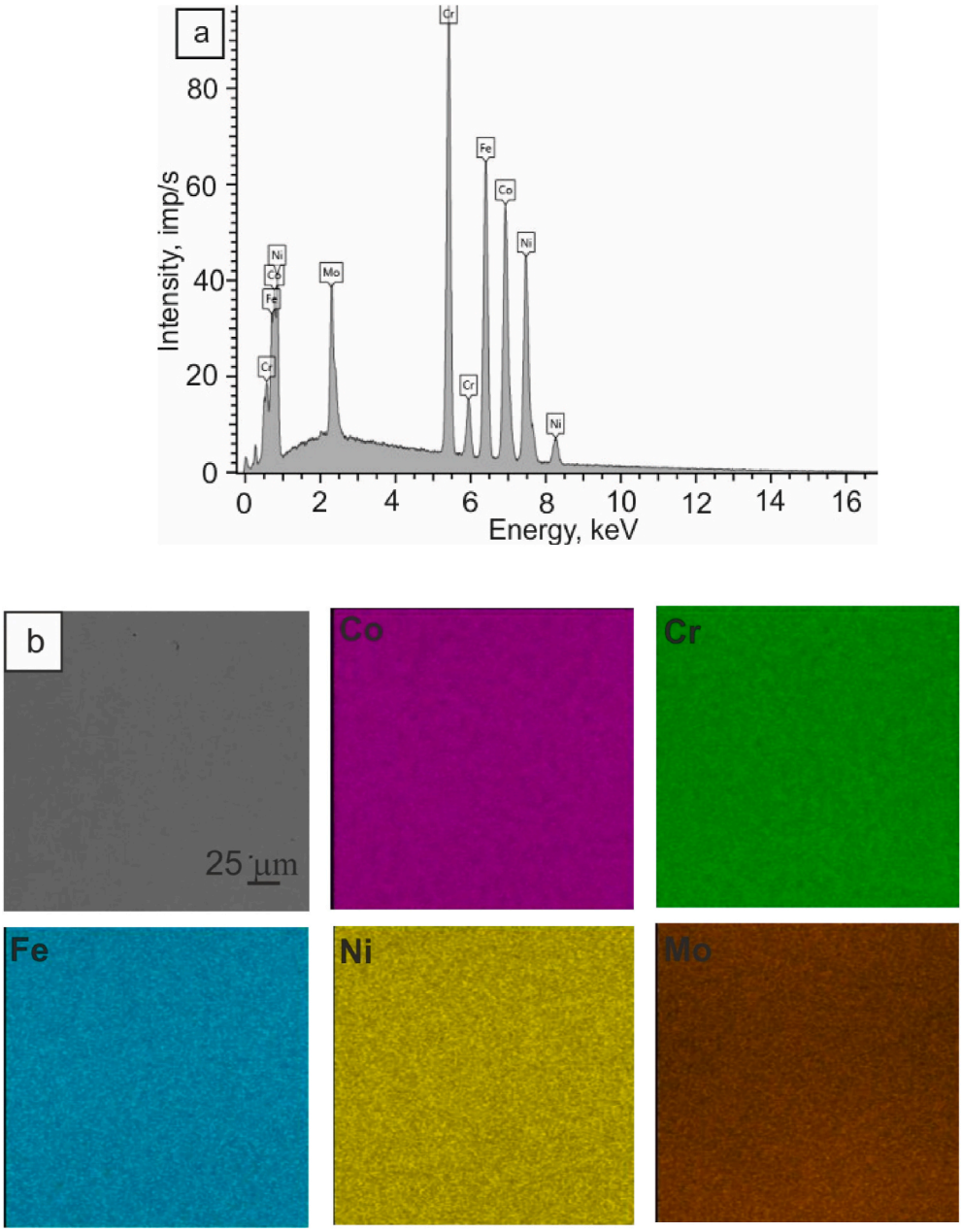

Fig. 2. Elemental composition (a) and SEM-EDS maps (b) showing homogeneous distribution of elements in the $CoCrFeNiMo_{0.2}$ HEA single crystals.

Table 1
Critical resolved shear stresses for slip in single crystals of fcc High Entropy Alloys (HEA) under tension.

Alloys	Temperature, K	Orientation		
		[001]	$[\bar{1}11]$	$[\bar{1}44]$
$CoCrFeNiMo_{0.2}$ HEA, single crystals in present paper	296	90 ± 2	88 ± 2	88 ± 2
	77	172 ± 2	174 ± 2	172 ± 2
Equiatomic CoCrFeMnNi HEA, single crystals [9]	296	82 ± 2	78 ± 2	80 ± 2
	77	155 ± 2	150 ± 2	156 ± 2
$CoCrFeNiAl_{0.3}$ HEA, single crystals [8]	296	86 ± 2	84 ± 2	
	77	162 ± 2	168 ± 2	

NiCoCr MEAs at 77 K [6,54–56]. Indeed, in the $[\bar{1}11]$-oriented $CoCrFeNiMo_{0.2}$ HEA crystals at 77 K, a planar dislocation structure develops, and splitting dislocations and isolated SFs are detected already after a low strain level of 5%. With an increase in strain up to 10–15%, large SFs and thin nanotwins with an average thickness of 5–10 nm are observed. Nanotwins develop between large SFs and multipoles (Fig. 4c–f). Analysis of microdiffraction patterns shows that reflections from twins have strands, indicating that the twins are thin (Fig. 4c–f). The $\sigma = 800 \pm 50$ MPa and, accordingly, $\tau_{cr}^{tw} = \sigma_{\varepsilon}{}^{*}m_{tw} = 250 \pm 15$ MPa are stresses, at which isolated SFs and thin nanotwins are detected in the study of the dislocation structure. In the $[\bar{1}11]$-oriented crystals, the m_{tw} does not change with strain levels since there is no precession of the crystal axis. Metallographically, on the surface of deformed samples, twins are found in two systems at $\varepsilon = 20\%$, with one prevailing (Fig. 4g). It can be seen that the twins form packets of large twins with thickness of 3.5–5 μm by overlapping nanotwins on top of each other. At lower strain levels, twinning is not observed metallographically.

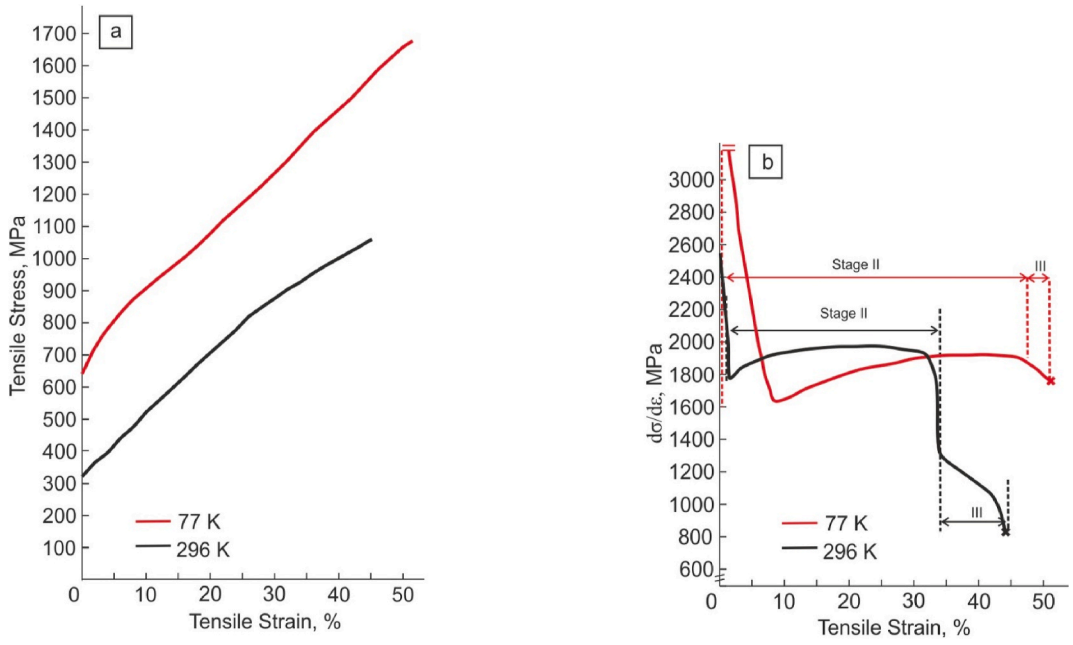

Fig. 3. (a) Tensile stress-strain response and (b) the evolution of strain hardening rate as a function of tensile strain in [$\bar{1}$11]-oriented single crystals of the CoCrFeNiMo$_{0.2}$ high-entropy alloy.

Usually, in fcc pure metals and their substitutional alloys with low γ_0, twins were observed metallographically on the surface of deformed samples when the deformation mechanism changed from slip to macrotwinning [26–28]. Therefore, the detecting of metallographic twins on the surface of the deformed [$\bar{1}$11]-oriented CoCrFeNiMo$_{0.2}$ HEA crystals may indicate a change in the deformation mechanism from slip to macrotwinning, and twinning can be considered as the main deformation mechanism in these crystals after strain of 20%. The $\sigma = 1080 \pm 50$ MPa, and, accordingly, $\tau_{cr}^{tw} = \sigma_\varepsilon * m_{tw} = 335 \pm 15$ MPa are stresses, at which the transition to macrotwinning is detected in the [$\bar{1}$11]-oriented CoCrFeNiMo$_{0.2}$ HEA crystals. These stresses can be considered as the twin propagation stresses, which are 1.34 times higher than the nanotwin nucleation stresses. In the [$\bar{1}$11]-oriented equiatomic CoCrFeMnNi HEA crystals at 77 K, twinning developed more intensively than in the [$\bar{1}$11]-oriented CoCrFeNiMo$_{0.2}$ HEA crystals, which is due to the difference in the γ_0 value ($\gamma_0 = 0.027$ J/m^2 in CoCrFeNiMo$_{0.2}$ HEA crystals and $\gamma_0 = 0.019$–0.021 J/m^2 in CoCrFeMnNi HEA [3,6,52]). Thus, the combination of high values of $\sigma_{0.1}$, due to the strong temperature dependence of $\sigma_{0.1}$(T), with $\gamma_0 = 0.027$ K J/m^2 leads to the development of twinning simultaneously with slip in CoCrFeNiMo$_{0.2}$ HEA crystals after strain of 5% at 77 K. At 77 K, in the [$\bar{1}$11]-oriented CoCrFeNiMo$_{0.2}$ HEA crystals, the Θ(ε) dependence with an increase in strain level is determined by the development of deformation by twinning and slip. With the development of deformation by twinning simultaneously with slip, plasticity reaches 52%, which is 7% higher than at 296 K, when deformation develops only by slip (Fig. 3).

3.3. *Tensile behaviour of* [$\bar{1}$44]*-oriented single crystals*

Fig. 5 shows the σ(ε) curves and the variation in the strain hardening coefficient $\Theta = d\sigma/d\varepsilon$ with tensile strain at 77 and 296 K of the CoCrFeNiMo0.2 HEA single crystals oriented along the [$\bar{1}$44] direction. In contrast to [$\bar{1}$11] orientation, oriented for multiple slip, the [$\bar{1}$44]-oriented crystals are oriented for shear in one system for slip or twinning. In the [$\bar{1}$44]-oriented crystals, the onset of plastic flow is characterized by a yield point (i.e., instability of plastic deformation) at both test temperatures. After the yield point, the plastic flow develops in three stages at 296 K, which are typical for slip deformation of fcc crystals oriented for a single slip [50,51]. The σ(ε) curve has a more complex staging at 77 K. The change in Θ with an increase in strain level also depends on the test temperature, as in [$\bar{1}$11]- oriented crystals (Figs. 3b and 5b).

At 296 K, in [$\bar{1}$44]-oriented crystals, the change in Θ with increasing strain levels is determined by the number of active slip systems. From the very beginning of the strain, Θ has negative values, which is associated with a small yield point. Then, at ε>2.5%, Θ becomes equal to zero, and at ε>5%, an increase in Θ to 1380 MPa is observed at ε = 52%. Studies of the precession of the crystal axis show that, under tensile strain from 10 to 60%, the [$\bar{1}$44] crystal axis moves in the [$\bar{1}$01] direction (Fig. 6a), which is the shear direction for slip in the primary slip system [$\bar{1}$01] (111) [28,38,50,51]. Consequently, from the very beginning, up to strain of 60%, plastic flow in [$\bar{1}$44]-oriented crystals develops via slip mainly in the primary slip system. At 296 K, slip is the main mechanism of deformation in crystals of this orientation. This is confirmed both optical metallography and TEM studies (Fig. 7a and b).

The change of the orientation of the crystal axis (precession) during strain makes it possible to determine the $\varepsilon_{X\text{-ray}}$ deformation calculated from the precession under the assumption that a single slip acts in the primary slip system [$\bar{1}$01] (111) according to the relation [38,51]:

$$\varepsilon_{X-ray} = \frac{\sin\lambda_0}{\sin\lambda_1} - 1 \quad (1)$$

here, λ_0 and λ_1 are the angles between the shear direction in the slip or twinning plane and the crystal axis before and after strain, respectively. A comparison of the given tensile strain ε with the $\varepsilon_{X\text{-ray}}$ strain calculated from the change in the precession of the crystal axis, under the assumption that slip is acting in the primary slip system [$\bar{1}$01] (111), is shown in Fig. 6c. The dotted line in Fig. 6c, inclined at an angle of 45° to the coordinate axes, corresponds to the condition under which $\varepsilon = \varepsilon_{X\text{-ray}}$ [51]. The values of $\varepsilon_{X\text{-ray}}$ calculated by relation (1) are below this straight line. Consequently, with the predominant development of slip in the primary slip system, slip also develops in the secondary system. This is consistent with an increase in Θ with an increase in strain up to 50%. At ε>55%, Θ decreases (Fig. 5b) and there is a transition to stage III of the dynamic recovery [50,51]. Plasticity reaches 70% at 296 K.

At 77 K, a more complex Θ(ε) dependence is observed in the [$\bar{1}$44]-oriented crystals than at 296 K. From the beginning of strain, Θ has

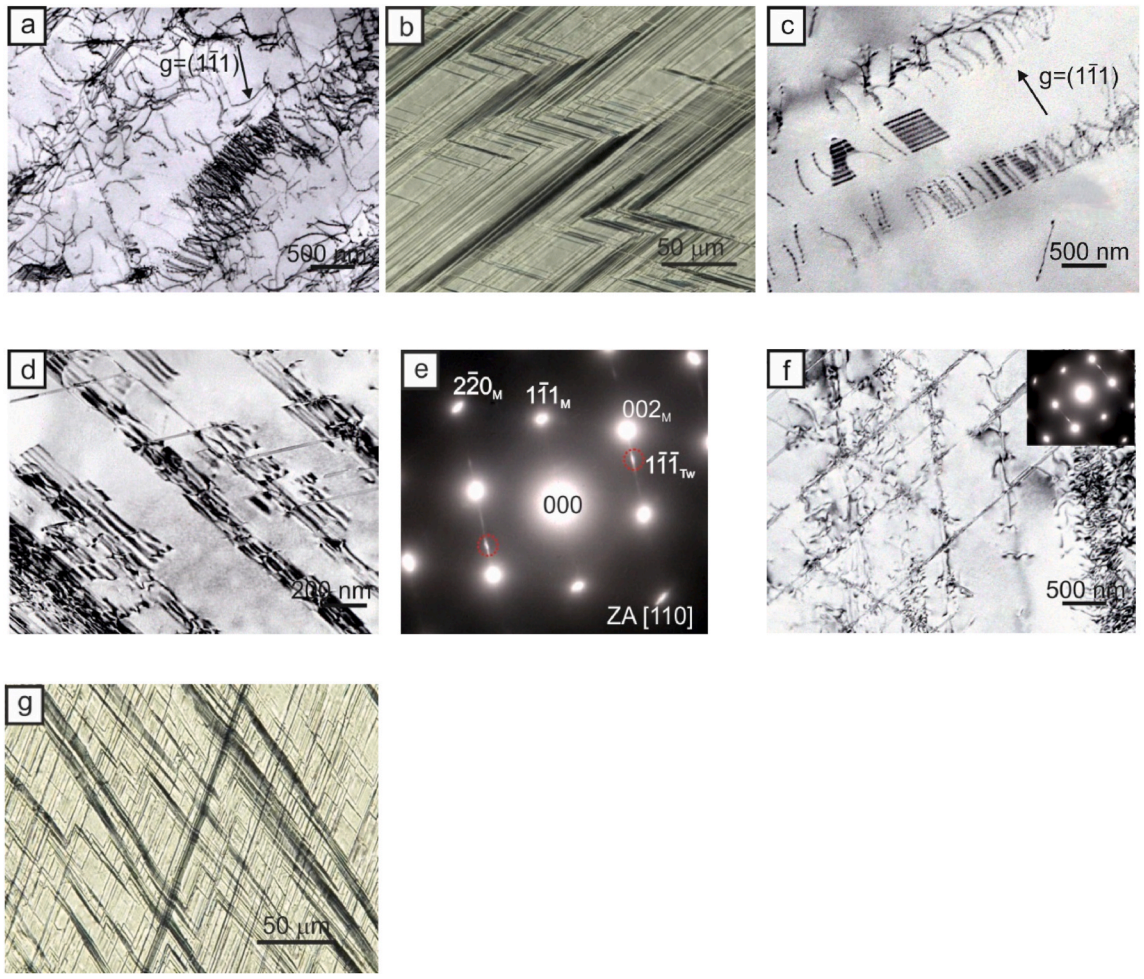

Fig. 4. TEM and optical images showing mechanism of deformation in the [$\bar{1}$11]-oriented single crystals of the $CoCrFeNiMo_{0.2}$ high-entropy alloy under tensile strain: (a) - Planar dislocation structure after strain of 5% at 296 K; (b) – Slip lines in the sample surface after strain of 20% at 296 K; (c) – Splitting dislocations and stacking faults after strain of 5% at 77 K; (d) – Large stacking faults and thin twins after strain of 10% at 77 K; (e) – Corresponding diffraction pattern for (d); (f) – Thin twins between multipoles after strain of 10% at 77 K with corresponding diffraction pattern; (g) - Twinning in the sample surface after strain of 20% at 77 K.

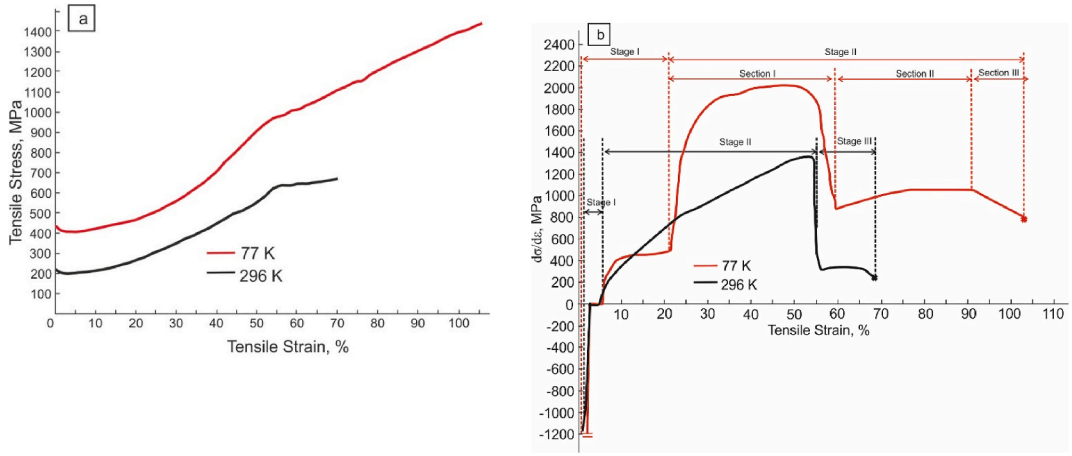

Fig. 5. (a) Tensile stress-strain response and (b) the evolution of strain hardening rate as a function of tensile strain in [$\bar{1}$44]-oriented single crystals of the $CoCrFeNiMo_{0.2}$ high-entropy alloy.

negative values, as at 296 K, which is associated with a small yield point. In the strain range from 3 to 20%, stage I of easy glide is observed, in which, at ε>2.5%, plastic deformation develops with a Lüders band with $\Theta = 0$ up to 5% strain. Then, at ε>5%, the deformation develops with a constant Θ = 450 MPa. At ε>20%, there is a transition to the linear stage, where Θ changes nonmonotonically. Initially, it sharply increases to 2000 MPa at 50%, and, at ε>50%, it sharply decreases to 900 MPa at strain of 60%. Onward, with increasing strain, Θ increases again to 1050

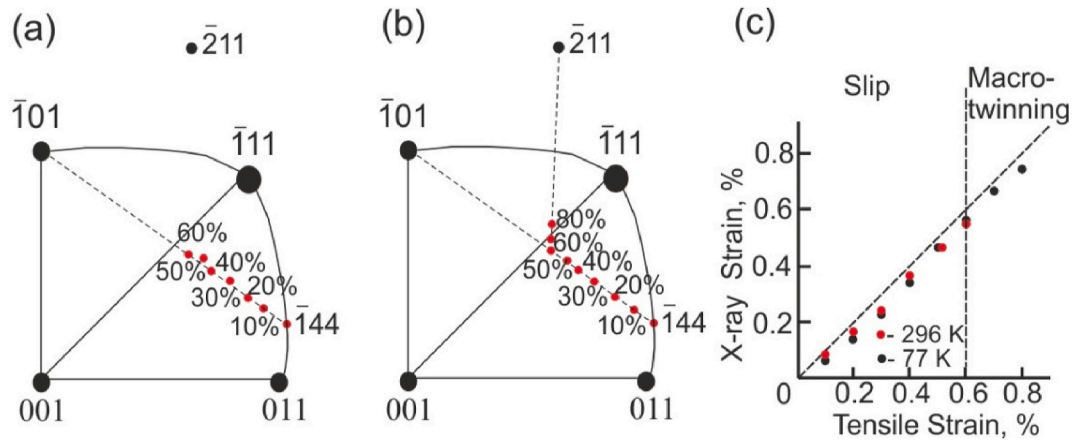

Fig. 6. Precession of crystal axis at 296 K (a) and 77 K (b), showing, respectively, the development of deformation by slip and twinning mainly in one system, and the $\varepsilon_{X\text{-}ray}$ deformation calculated from the precession of crystal axis (c) for [$\bar{1}$44]-oriented single crystals of the $CoCrFeNiMo_{0.2}$ high-entropy alloy under tensile strain.

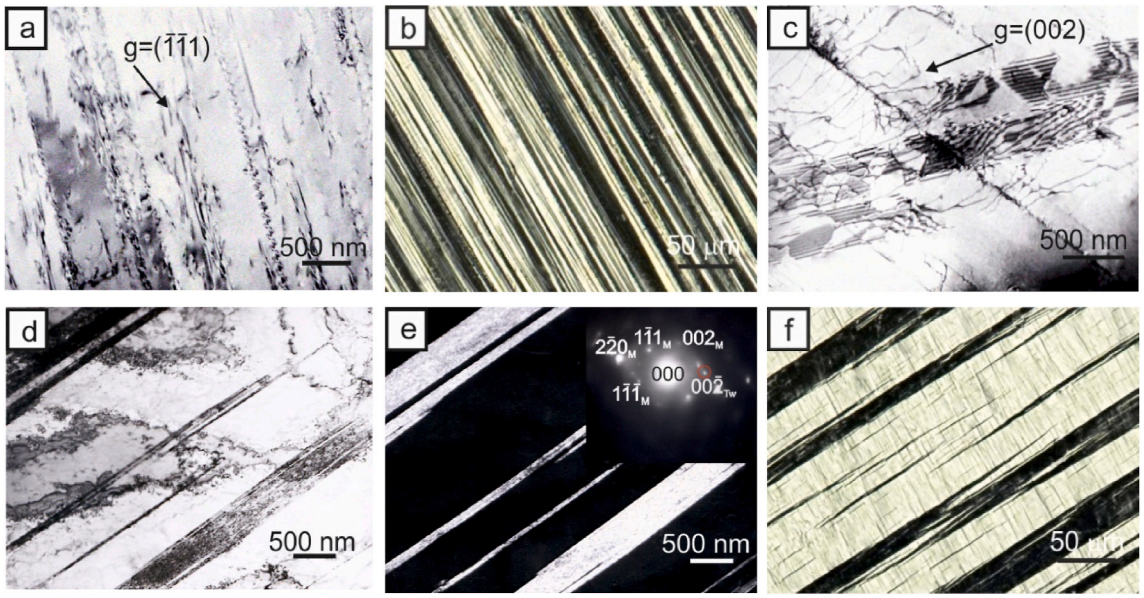

Fig. 7. TEM and optical images showing mechanism of deformation in the [$\bar{1}$44]-oriented single crystals of the $CoCrFeNiMo_{0.2}$ high-entropy alloy under tensile strain: (a) - Planar dislocation structure after strain of 15% at 296 K; (b) – Slip lines in the sample surface after strain of 40% at 296 K; (c) – Dislocations and stacking faults after strain of 5% at 77 K; (d) – Twinning in one system after strain of 60% at 77 K; (e) - Dark-field image of twinning with corresponding diffraction pattern after strain of 60% at 77 K; (f) – Twinning in one system in the sample surface after strain of 60% at 77 K.

MPa at $\varepsilon = 70\%$ and remains constant up to 95%, and then decreases again (Fig. 5b). Such a multi-stage $\Theta(\varepsilon)$ dependence with increasing strain was previously observed in [011]-, [$\bar{1}$11]- and [$\bar{1}$23]-oriented NiCoCr MEA crystals at 77 K via simultaneous development of twinning and slip deformation [57]. To elucidate the physical reason of the complex $\Theta(\varepsilon)$ dependence in the [$\bar{1}$44]-oriented $CoCrFeNiMo_{0.2}$ HEA crystals at 77 K, the precession of the crystal axis is studied (Fig. 6b). As can be seen from Fig. 6b, at 77 K, the [$\bar{1}$44] crystal axis of the sample initially moves in the [$\bar{1}$01] direction up to strain of 60%, which is the shear direction for slip in the primary slip system [$\bar{1}$01] (111) [38,51]. Consequently, at 77 K up to 60% strain, the deformation mechanism is governed by slip, which is the main mechanism of deformation [9,50, 51]. Then, at tensile strain $\varepsilon \geq 60\%$, the [$\bar{1}$44] crystal axis changes direction and moves in the [$\bar{2}$11] direction, i.e., the direction of shear for twinning in the primary twin system [$\bar{2}$11] (111) (Fig. 6b) [9,26,28,38]. This means that twinning develops predominantly in the primary [$\bar{2}$11] (111) twinning system and is the main deformation mechanism in these crystals after strain of 60% at 77 K. Both optical metallography and TEM studies (Fig. 7) confirm these changes in the precession of the crystal axis, indicating a change in the deformation mechanism from slip to twinning with increasing strain levels. At 77 K, in [$\bar{1}$44]-oriented crystals, as well as in [$\bar{1}$11]-oriented crystals, SFs are observed after strain of 5% (Fig. 7c). Twinning in one system take place after strain of 20%, but is not yet detected metallographically on the surface of the deformed samples, since the twins are thin with a thickness of 10–15 nm on the average. The values of $\varepsilon_{X\text{-}ray}$ calculated by relation (1), when slip and thin nanotwins develop simultaneously at 77 K, are lower than at 296 K with the development of deformation only via slip (Fig. 6c). Consequently, at strain levels from 20 to 30%, a sharp increase in Θ is determined by the nanotwins-slip interaction, when slip develops predominantly in the primary [$\bar{1}$01] (111) slip system. At a tensile strain of 60%, when a decrease in Θ is observed on the $\sigma(\varepsilon)$ and $\Theta(\varepsilon)$ dependences and the crystal axis moves in the [$\bar{2}$11] direction, twins predominantly in one system are detected both in the TEM and optical images when studying of the dislocation structure and the surface of deformed crystals

(Fig. 7d–f). In this case, the difference between the ε and $\varepsilon_{X\text{-ray}}$ values decreases compared to a lower strain levels (Fig. 6c). This qualitatively confirms the development of twinning mainly in the primary $[\bar{2}11]$ (111) twinning system [28,38], and this is consistent with a decrease in Θ and an increase in plasticity (Fig. 5). According to TEM data, the thickness of twins varies from 100 to 600 nm (Fig. 7d and e). At 77 K, the plasticity reaches 106% and becomes 1.5 times greater than at 296 K with only slip deformation (Fig. 5a).

Both TEM and X-ray studies make it possible to determine the CRSS for twinning in the $[\bar{1}44]$-oriented $CoCrFeNiMo_{0.2}$ HEA crystals. TEM studies of large SFs and nanotwins in $[\bar{1}44]$-oriented crystals at 77 K are found after strain of 20% at stresses $\sigma = 450 \pm 50$ MPa and, accordingly, $\tau_{cr}^{tw} = \sigma_\varepsilon * m_{tw} = 212 \pm 25$ MPa ($m_{tw} = 0.47$ taking into account precession of the crystal axis). X-ray shows that twinning, as the main mechanism of deformation, develops after strain of 60% at $\sigma = 1000 \pm 50$ MPa and, accordingly, $\tau_{cr}^{tw} = 400 \pm 25$ MPa ($m_{tw} = 0.4$ considering precession of the crystal axis). The τ_{cr}^{tw} for twinning, determined from X-ray, may be considered as the stresses for twinning propagation. As for τ_{cr}^{tw} at which twins are observed only according to TEM, they may be taken as stresses for the nucleation twinning, since twinning is not the main mechanism of deformation at these stresses. In $[\bar{1}44]$-oriented crystals, τ_{cr}^{tw} for twin propagation is almost two times higher than τ_{cr}^{tw} for nucleation. Therefore, twinning in fcc $CoCrFeNiMo_{0.2}$ HEA is controlled by the propagation process, as in high-strength austenitic steels, Hadfield steels and polycrystals of the equiatomic CrFeNi MEA [32,38,56]. It should be noted that, in $[\bar{1}44]$-oriented crystals, twins appear on the surface of deformed samples at the moment when the crystal axis changes the direction of motion from $[\bar{1}01]$ to $[\bar{2}11]$ in the study of precession. Consequently, the metallographic detection of twins on the sample surface may indicate, as well as the precession of the crystal axis, the transition to the development of deformation by macrotwinning. In the $[\bar{1}11]$-oriented crystals, there is no precession of the crystal axis, since slip develops simultaneously in several systems. Therefore, in the $[\bar{1}11]$-oriented crystals, the transition to the development of deformation by macrotwinning can be recorded metallographically by the appearance of twins on the surface of the samples at strain of 20%.

3.4. Tensile behaviour of [001]-oriented single crystals

Fig. 8 shows the σ(ε) curves and the variation in the strain hardening coefficient $\Theta = d\sigma/d\varepsilon$ with tensile strain at 77 and 296 K of the CoCrFeNiMo0.2 HEA single crystals oriented along the [001] direction. The [001]-oriented crystals, like $[\bar{1}11]$-oriented crystals, are oriented for multiple slip. The behavior of the σ(ε) and Θ(ε) curves shows that the plastic flow begins from stage II of linear hardening at both test temperatures (Fig. 8), as in fcc pure metals and their substitutional alloys oriented for the development of slip deformation in several systems [50,51]. In the [001]-oriented crystals, Θ increases linearly with an increase in strain levels and weakly depends on the test temperature, which is typical for slip deformation (Fig. 8b) [8,50,51]. At 77 and 296 K, a planar structure develops. The strain at the stage of linear hardening is governed only by slip (Fig. 9), and twinning is not detected. Earlier, in [001]-oriented crystals of the equiatomic CoCrFeMnNi HEA with a lower $\gamma_0 = 0.018$–0.022 J/m^2 than in $CoCrFeNiMo_{0.2}$ HEA with $\gamma_0 = 0.027$ J/m^2, twinning was found by the mechanism of nucleation and growth of extrinsic SFs under tensile strain at 77 K [33]. With the development of twinning with slip, Θ in the [001]-oriented CoCrFeMnNi HEA crystals [33], as well as in the $[\bar{1}11]$-oriented $CoCrFeNiMo_{0.2}$ HEA crystals (Fig. 3) was higher than in the case of deformation only by slip in the [001]-oriented $CoCrFeNiMo_{0.2}$ HEA crystals. As soon as stage II is completed in [001]-oriented crystals, a decrease in Θ is observed (Fig. 8b), and a transition occurs to stage III of dynamic recovery [8,50,51]. The transition to stage III of dynamic recovery occurs at strain of 30% at 296 K and at strain of 35% at 77 K. In the [001]-oriented crystals under slip deformation, plasticity is close at both temperatures and amounts to 37 and 35%, respectively, at 77 and 296 K and is lower than that of the $[\bar{1}11]$- and $[\bar{1}44]$-oriented crystals under twinning deformation.

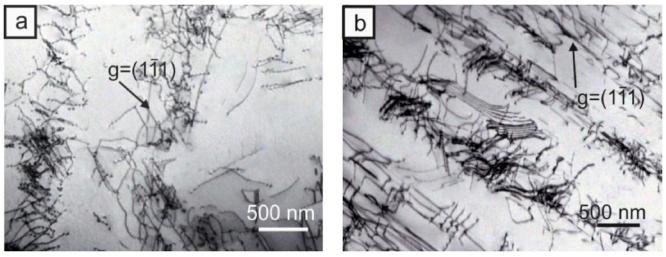

Fig. 9. Planar dislocation structure in [001]-oriented single crystals of the $CoCrFeNiMo_{0.2}$ high-entropy alloy under tensile strain: (a) - after strain of 5% at 296 K; (b) - after strain of 10% at 77 K.

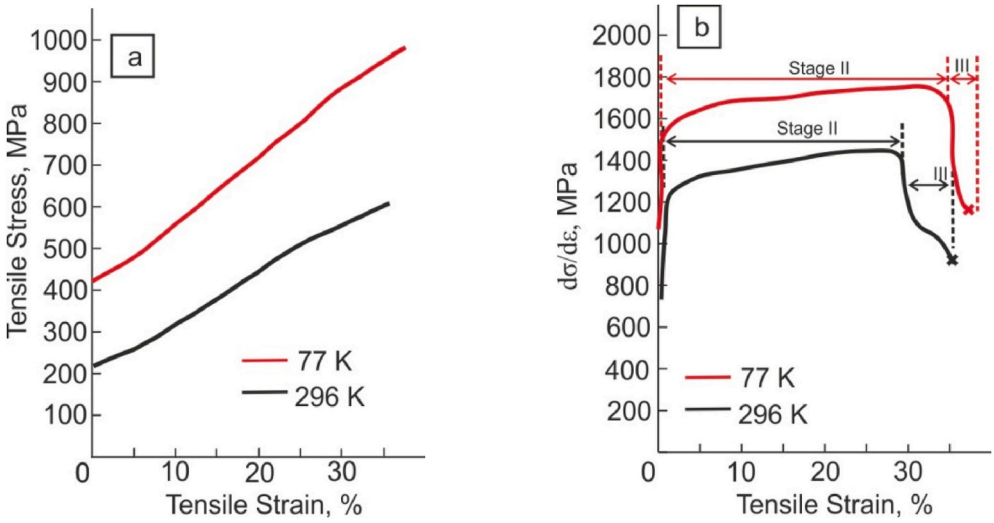

Fig. 8. (a) Tensile stress-strain response and (b) the evolution of strain hardening rate as a function of tensile strain in [001]-oriented single crystals of the $CoCrFeNiMo_{0.2}$ high-entropy alloy.

4. Discussion

4.1. Critical resolved shear stress for twinning in $CoCrFeNiMo_{0.2}$ HEA single crystals

Analysis of the literature data showed that, in fcc structures, the transition to twinning deformation occurred when the CRSS τ_{cr}^{tw} for twinning was reached in the twinning plane. It is important to note that the development of twinning in fcc structures strongly depends on the solid solution concentration, value of γ_0, crystal orientation, strain rate, and test temperature [12,26–36]. Thus, in pure metals, for instance, silver (Ag) with a stacking fault energy $\gamma_0 = 0.03$ J/m^2 close to γ_0 for the $CoCrFeNiMo_{0.2}$ HEA single crystals, twinning developed at low temperatures after a significant strain level. The transition to twinning was accompanied by a sharp decrease in stresses on the σ(ε) curve, and the slip deformation was completely suppressed. The twins propagated along the crystal in a Lüders band and were detected metallographically on the surface of the deformed samples. The stresses for the nucleation and propagation of twins were close [26–28]. A similar development of twinning was observed in dilute solid solutions, for example, Ag-(1–4) at.% In Ref. [28]. In concentrated solid solutions, such as Cu-8 at.% Ge, Cu-8 at.% Al, Ag-8 at.% In, austenitic stainless steels with nitrogen, Hadfield steels, etc. [26–28,32,34,38], an increase in the concentration of the alloying element led to a decrease in γ_0, the development of a planar dislocation structure and the facilitation of deformation by twinning. In these concentrated solid solutions, the σ(ε) curves did not show a decrease in stresses corresponding to the onset of twinning, and the Lüders band of twin propagation was not observed. As a result, it was not possible to determine the stresses for the nucleation and propagation of twins on the σ(ε) curves without TEM and X-ray studies. Plastic deformation developed with hardening due to the simultaneous development of twinning and slip and led to the appearance of the TWIP-effect [12,31,38]. In the case of concentrated solid solutions, twins were very thin and were not observed metallographically on the surface of deformed samples, in contrast to pure metals and dilute solid solutions. In concentrated solid solutions, twins were easily generated, but their propagation was difficult. Such a difference in the nucleation and propagation of twins was associated with the influence of SRO, which increased the resistance to the motion of perfect and twinning dislocations [8,9,41–45].

In fcc metals and their substitutional alloys, the τ_{cr}^{tw} depended on the crystal orientation. Under tensile strain, the lowest τ_{cr}^{tw} were observed in [$\bar{1}$11]-oriented crystals, which increased with the deviation from [$\bar{1}$11] orientation to [001] orientation [28,29]. The τ_{cr}^{tw} did not depend on the test temperature when twinning developed at stage II of linear hardening and depended on temperature if twinning developed at stage III of the σ(ε) curve [28,29].

The experimental data obtained in the present paper showed that in the [$\bar{1}$11]- and [$\bar{1}$44]-oriented $CoCrFeNiMo_{0.2}$ HEA crystals, twinning turned out to be a low-temperature deformation mechanism, namely, it developed at 77 K, and was not observed at 296 K, in contrast to single crystals of the equiatomic CoCrFeMnNi HEA [9]. Single crystals of both $CoCrFeNiMo_{0.2}$ and CoCrFeMnNi HEAs are characterized by close values of τ_{cr}^{sl} (Table 1). The absence of twinning in the [$\bar{1}$11]-and [$\bar{1}$44]-oriented $CoCrFeNiMo_{0.2}$ HEA crystals at 296 K is due to the higher γ_0 than in CoCrFeMnNi HEA ($\gamma_0 = 0.027$ J/m$_2$ in $CoCrFeNiMo_{0.2}$ HEA and $\gamma_0 =$ 0.018–0.022 J/m^2 in CoCrFeMnNi HEA [3,6,52]) and SRO in the arrangement of Mo atoms in the $CoCrFeNiMo_{0.2}$ HEA single crystals and its absence in the CoCrFeMnNi HEA single crystals [8,9,53]. The SRO in $CoCrFeNiMo_{0.2}$ HEA is qualitatively confirmed by the development of a planar dislocation structure with dislocation pile-ups in [001]- and [$\bar{1}$11]-oriented crystals at 296 K at a strain of 5% (Figs. 4a and 9a), which was not observed in crystals of these orientations of the CoCrFeMnNi HEA under the same conditions [53]. At 296 K, in the deformed [001]- and [$\bar{1}$11]-oriented crystals of the equiatomic CoCrFeMnNi HEA up to 5%, the dislocation structure was a uniform distribution of dislocations without pile-ups [53]. As in concentrated fcc crystals, in the studied orientations of $CoCrFeNiMo_{0.2}$ HEA, when deformation developed by twinning, the σ(ε) curves did not show a decrease in stresses corresponding to the onset of twinning, and the Lüders band of twin propagation was not observed. However, in the [$\bar{1}$11]- and [$\bar{1}$44]-oriented $CoCrFeNiMo_{0.2}$ HEA crystals, in contrast to concentrated solid solutions, two types of twins were found. The first type is thin nanotwins with thickness of 5–10 nm, which are detected only by TEM in the study of the dislocation structure at low strain level. The second type is macrotwins, when both optical metallography and X-ray studies reveal twinning as the main mechanism of deformation in studying the surface of deformed crystals and the precession of the crystal axis (Figs. 4g, 6b and 7f). When nanotwins appeared on the σ(ε) curves, plastic deformation developed with high Θ (up to 10% in [$\bar{1}$11]-oriented crystals and up to 50% in [$\bar{1}$44]-oriented crystals) due to the nanotwins-slip interaction, and the TWIP-effect was observed (Figs. 3 and 5). The transition to macrotwinning was accompanied by a notable decrease in Θ due to the predominant development of twinning in one system and a decrease in the contribution of slip to strain hardening, which was especially evident in [$\bar{1}$44]-oriented crystals (Fig. 5).

The development of thin nanotwins after a low strain level by slip, which are detected only by TEM, can occur via a Copley-Kear-Byun "glide source" mechanism [12,32,33,58,59], when perfect dislocations a/2<110> (b) are split into the partial Shockley dislocations a/6<112> (b_1 and b_2) according to the Heidenreich-Shockley reaction in the (111) plane:

$$a/2\langle 101\rangle \geq a/6\langle 211\rangle + a/6\langle 112\rangle \quad (2)$$

$$b = b_1 + b_2$$

The value of the splitting of perfect dislocation a/2<110> depends on the level of external stresses, the crystal orientation and the method of deformation (tension and compression) according to the relation [58]:

$$d = \frac{Gb_1^2}{8\pi\gamma_{ef}};\ \gamma_{ef} = \gamma_0 \pm \frac{(m_2 - m_1)}{2}\sigma b_1 \quad (3)$$

here G is shear modulus of HEA, b_1 is the Burgers vector modulus of a partial Shockley dislocation, $Q = \frac{(m_2 - m_1)}{2}$ is the orientation factor, where m_1 and m_2 are Schmid factors for leading b_1 and trailing b_2 Shockley dislocations, respectively, σ is the applied stress and ± takes the sign of the applied stress, i.e. tension or compression, into account, γ_{ef} is the effective stacking fault energy, which depends on the value of γ_0, the magnitude of the applied stresses σ and the orientation factor Q [32,58]. An analysis of relation (3) shows that, in the case of tensile strain, in order to realize the "glide source", it is necessary to decrease γ_{ef} in the field of external stresses. This is achieved when the external stresses and hence the Schmid factor m_1 for the twinning dislocation b_1 is greater than m_2 for the trailing dislocation b_2, $m_1 > m_2$ and $Q < 0$ [32,33,58]. In [$\bar{1}$11]- and [$\bar{1}$44]-oriented crystals, the Q value is −0.08 and −0.13, respectively [58]. As the stress increases, γ_{ef} decreases and may differ from the equilibrium γ_0 value by more than two times. In the [$\bar{1}$11]- и [$\bar{1}$44]-oriented $CoCrFeNiMo_{0.2}$ HEA crystals at 77 K, the first isolated STs and nanotwins were observed at strain of 5–10%, respectively, at the stress levels of 800 and 470 MPa. According to relation (3), at the experimentally-determined value of $\gamma_0 = 0.027$ J/m^2 for $CoCrFeNiMo_{0.2}$ HEA crystals, isolated STs and nanotwins appear in [$\bar{1}$44]-oriented crystals with $Q = -0.13$, when $\gamma_{ef} = 0.018$ J/m^2, and in [$\bar{1}$11]-oriented crystals with $Q = -0.08$ at $\gamma_{ef} = 0.017$ J/m^2. The value of dislocation splitting, according to relation (3), on the contrary, increases to 4.2 and 4.5 nm, respectively, in [$\bar{1}$44]- and [$\bar{1}$11]-oriented crystals relative to the equilibrium value of dislocation splitting $d_0 = 2.8$ nm, corresponding to $\gamma_0 = 0.027$ J/m^2. As a result, the dislocation structure becomes planar,

cross-slip processes are suppressed and intrinsic SFs appear due to the splitting of perfect a/2<110> dislocations into partial a/6<112> Shockley dislocations, the layering of which leads to the growth of twins in thickness [9,12,26–29,32,33]. It should be noted that in the heavy distorted crystal lattice of the fcc HEAs, the mobility of partial Shockley dislocations is higher than that of perfect dislocations, since partial Shockley dislocations are mixed or screw and weakly interact with substitutional atoms [8,60,61]. This fact also contributes to the nucleation of nanotwins after the low strain levels by slip according to the "glide source" mechanism, which was previously observed in CoCrFeMnNi HEA single crystals [9,33].

CRSS τ_{cr}^{tw} for nanotwinning, taking into account the change in γ_{ef} after a low strain levels by slip, can be determined from the relation [12,26,28,33]:

$$n\tau_{cr}^{tw} = \frac{\gamma_{ef}}{b_1} + \tau_f(b_1) + \alpha m_{sl}\ Gb\rho^{1/2} \quad (4)$$

here $\frac{\gamma_{ef}}{b_1}$ is the stress, which is necessary for the generation of the first intrinsic SF in the HEA [62], $\tau_f(b_1)$ is the frictional stress experienced by the partial Shockley dislocation during its movement in the CoCrFeNiMo$_{0.2}$ matrix, $\alpha m_{sl}Gb\rho^{1/2}$ is the stress at strain hardening at deformation by slip to twinning (α is constant [63], m_{sl} is the Schmid factor for slip in the primary slip plane, $G = 85$ GPa [64] is the shear modulus of HEA at 77 K, b = 0.25 нМ is the Burgers vector modulus of a perfect dislocation a/2<110>, ρ is the dislocation density), n = 1–4 is the stress concentrator for twin nucleation [12,63].

CRSS τ_{cr}^{sl} for slip after a low strain levels is determined by the relation:

$$\tau_{cr}^{sl} = \tau_f(b) + \alpha m_{sl} Gb\rho^{1/2} \quad (5)$$

here $\tau_f(b)$ is the frictional stress experienced by the perfect dislocation during its movement in the CoCrFeNiMo$_{0.2}$ HEA matrix. To estimate τ_{cr}^{tw} by relation (4), the value of $\tau_f(b_1)$ is taken equal to $\tau_{cr}^{sl} = 172$ MPa at 77 K, which does not depend on the crystal orientation (Table 1). Since partial Shockley dislocations are mixed or screw [61] and weakly interact with substitutional atoms, then $\tau_f(b_1)$ can be less than 172 MPa. The value of $\alpha m_{sl}Gb\rho^{1/2}$ is determined from the $\sigma(\varepsilon)$ curve as $\Delta\tau = m_{sl}(\sigma_\varepsilon - \sigma_{0.1})$ ($\sigma_{0.1}$ and σ_ε, are, respectively, stresses at the yield point and at a strain of 5% and 20%, at which isolated SFs and nanotwins appear in [$\bar{1}$11]- and [$\bar{1}$44]-oriented crystals, respectively). The $\Delta\tau$ are equal to 40.5 and 16 MPa for [$\bar{1}$11]- and [$\bar{1}$44]-oriented crystals, respectively. The $\frac{\gamma_{ef}}{b_1}$ values are 113 and 120 MPa at $\gamma_{ef} = 0.017$ and 0.018 J/m^2, respectively, for [$\bar{1}$11]- and [$\bar{1}$44]-oriented crystals. Thus, for [$\bar{1}$11]- and [$\bar{1}$44]-oriented crystals, τ_{cr}^{tw} , estimated from equation (4), turned out to be equal to 325 and 308 MPa, respectively. The τ_{cr}^{tw} estimated by equation (4) coincided with the experimental values of τ_{cr}^{tw} for nanotwinning, determined from the stresses on the $\sigma(\varepsilon)$ curves at which nanotwins were observed by TEM, at n = 1 (Table 2). To estimate τ_{cr}^{sl} after low strain level at 77 K in the [$\bar{1}$11]- and [$\bar{1}$44]-oriented CoCrFeNiMo$_{0.2}$ HEA crystals, using equation (5), $\tau_f(b)$ is taken equal to $\tau_{cr}^{sl} = 172$ MPa at the yield point and $\Delta\tau$ equal to 40.5 and 16 MPa, as for twinning. For [$\bar{1}$11]- and [$\bar{1}$44]-oriented crystals, τ_{cr}^{sl} , estimated from equation (5), were equal to 212.5 and 188 MPa, respectively. Comparison of the estimated values according to relations (4) and (5) shows that $\tau_{cr}^{sl} < \tau_{cr}^{tw}$. Under this condition, the deformation mechanism does not change from slip to twinning [26–28]. At 77 K, due to the strong temperature dependence of τ_{cr}^{sl} (T) and solid solution hardening by Mo atoms, a planar structure with dislocation pile-ups develops. In the head of pile-up, local fields of internal stresses arise [28,33], which, in addition to external ones, contribute to the splitting of the perfect dislocation into the partial Shockley dislocations. As a result, nanotwins easily nucleate after a low strain levels, but do not grow.

With an increase in stresses σ with an increase in strain level, the γ_{ef}

Table 2
Critical resolved shear stresses for twinning τ_{cr}^{tw} in fcc HEAs and fcc pure metals depending on the stacking fault energy γ_0; T – temperature; G – shear modulus; TEM (Transmission electron microscopy), OM (Optical microscopy), X-ray, DIC (digital image correlation) - twin detection methods.

Alloys	γ_0, J/m^2	Orientation	T, K	τ_{cr}^{tw}, MPa	G, GPa	τ_{cr}^{tw}/G 10^3
CoCrFeNiMo$_{0.2}$ HEA single crystals in present paper	0.027	[$\bar{1}$11]	77	250 (TEM)	85	2.9
				335 (OM)		3.9
		[$\bar{1}$44]	77	221 (TEM)		2.7
				400 (OM, X-ray)		4.7
Equiatomic CoCrFeNiMn HEA single crystals [9]	0.018	[$\bar{1}$11]	296	110 (TEM)	81	1.35
			77	200 (TEM)	85	2.3
		[$\bar{1}$44]	296	110 (TEM)	81	1.35
			296	185 (X-ray)	81	2.3
			77	190 (TEM)	85	2.23
			77	190 (X-ray)	85	2.23
		[$\bar{1}$23]	296	135 (TEM)	81	1.7
			77	185 (TEM)	85	2.2
			77	325 (X-ray)	85	3.8
		[011]	77	155 (TEM)	85	1.9
			77	290 (X-ray)	85	3.4
		[001]	77	155 (TEM)	85	2.5
Equiatomic CoCrFeNiMn HEA single crystals [29,30]	0.018	[$\bar{1}$11]		164 (DIC)	85	1.9
		[$\bar{1}$44]	77	163 (DIC)		1.9
		[$\bar{1}$22]		153 (DIC)		1.8
$Fe_{40}Mn_{40}Cr_{10}Co_{10}$ HEA single crystals [54]	0.013	[$\bar{1}$11]	296	72 (DIC)	81	0.9
		[$\bar{1}$23]		70 (DIC)		0.86
CoCrFeNiAl$_{0.3}$ HEA single crystals [8]	0.051	[$\bar{1}$11]	77	295 (TEM)	85	3.5
Equiatomic CoCrFeNiMn HEA polycrystals with grain size d = 17 μm [37]	0.022		77	235 (TEM)	85	2.7
Equiatomic CrFeNi MEA polycrystals with grain size d = 34 μm [56]	0.037		293	170 (TEM)	81	2.09
			77	160 (TEM)	85	1.9
Ag single crystals [26,28]	0.030	[$\bar{1}$11]	293	77	30	2.4
			77	44		1.5
		[$\bar{1}$44]	77	50		1.7
Cu single crystals [26,28]	0.050	[$\bar{1}$11]	4.2	130	46	2.8

decreases, according to relation (3). At tensile strain of 20 and 60%, at which twinning is detected metallographically in [$\bar{1}$11]- oriented crystals and from the change in the precession of the crystal axis in [$\bar{1}$44]-oriented crystals, γ_{ef} is 0.014 and 0.007 J/m^2, respectively. With increasing stresses at high strain levels, the value of γ_{ef} decreased almost by a factor of two and four compared to γ_0, respectively, in [$\bar{1}$11]- and [$\bar{1}$44]-oriented crystals. This means that perfect dislocations lose their stability to splitting and there is a transition to an avalanche-like formation of STs and nanotwins (Fig. 10). Nanotwins that nucleate after a high strain level combine into twin packs, overcoming the SRO, in contrast to low strain levels, where they nucleate rather than grow. The γ_{ef} tends to zero, and a transition to the development of macrotwinning occurs. Estimation of τ_{cr}^{tw} for macrotwinning, using relation (4), shows that in [$\bar{1}$11]-oriented crystals at strain of 20%, when $\tau_f(b_1) = 172$ MPa, $\frac{\gamma_{ef}}{b_1} = 93$ MPa and $\Delta\tau = 116$ MPa, τ_{cr}^{tw} are equal to 381 MPa. In the [$\bar{1}$44]- oriented crystals at strain of 60%, when $\tau_f(b_1) = 172$ MPa, $\frac{\gamma_{ef}}{b_1} = 47$ MPa and $\Delta\tau = 236$ MPa, τ_{cr}^{tw} for macrotwinning are equal to 455 MPa. Estimates τ_{cr}^{sl} after high strain level at 77 K in the [$\bar{1}$11]- and [$\bar{1}$44]-oriented crystals, using equation (5), are equal to 288 and 408 MPa, respectively. The difference between the τ_{cr}^{sl} and τ_{cr}^{tw} values decreases with increasing stress. In the [$\bar{1}$44]-oriented crystals, where the change in the deformation mechanism from slip to twinning is determined by the precession of the crystal axis (Fig. 6b), $\tau_{cr}^{sl} \approx \tau_{cr}^{tw}$.

Previously, on polycrystals of austenitic stainless steels, Byun showed [59] that twinning is activated when the applied stress is high enough to initiate breakaway of partial dislocations, which appeared as a result of the splitting of screw dislocations. In the dislocation structure of the fcc HEAs, two types of dislocations have always been observed: non-splitting and splitting (Fig. 4c) [8,9,33,61]. Non-splitting dislocations were edge dislocations and the field of external stresses did not act on them, while splitting dislocations were screw or mixed and, on the contrary, the field of external stresses acted on them. The maximum change in the splitting value was experienced by screw dislocations [8, 59,61,65]. A high level of stresses is required for the breakaway and sliding of the first partial dislocation. As soon as the first SF was formed upon the breakaway of the first partial dislocation, the stress for the further development of twinning decreased [59]. The applied stress at which the breakaway of partial dislocations occurs can be considered as the axial stress for macrotwinning σ_{tw}, which, according to Ref. [59], can be determined by the relationship:

$$\sigma_{tw} = 6.14\frac{\gamma_0}{b_1} \tag{6}$$

It can be seen from relation (6) that σ_{tw} is a function of γ_0 and b_1. In the CoCrFeNiMo$_{0.2}$ HEA single crystals, according to relation (6), at $\gamma_0 = 0.027$ J/m^2, the σ_{tw} should be equal to 1100 MPa. In [$\bar{1}$44]-oriented crystals, this stress level is reached at strain of 68%. This is in good agreement with the data of the precession of the crystal axis, when, at strain of 60% and the corresponding stress level of 1020 MPa, the crystal axis changed direction from slip to twinning. In [$\bar{1}$11]-oriented crystals, $\sigma_{tw} = 1100$ MPa is achieved at strain of 22%, at which twinning is detected metallographically on the surface of deformed crystals (Fig. 4g).

According to Ref. [59] and considering the dependence of the γ_0 value on the external stress level and the crystal orientation (relation (3)) [58], the τ_{cr}^{tw} for macrotwinning can be defined as the critical stress at which the breakaway of partial dislocations occurs, according to the relation:

$$\tau_{cr}^{tw} = \frac{2\gamma_{ef}}{b_1} \tag{7}$$

To convert σ_{tw} in relation (6) into τ_{cr}^{tw} for macrotwinning, we used the average Schmid factor for twinning $m_{tw} = 0.326$ in polycrystals [58,59]. For the [$\bar{1}$11]-oriented crystals, the τ_{cr}^{tw} for macrotwinning, estimated with using equation (7) and $\gamma_{ef} = 0.014$ J/m^2 at strain of 20%, results in 186 MPa. As for the [$\bar{1}$44]-oriented crystals, an estimate of the τ_{cr}^{tw} for macrotwinning, using equation (7) and $\gamma_{ef} = 0.007$ J/m^2 at strain of 60%, results in 93 MPa. In this case, $\tau_{cr}^{tw} < \tau_{cr}^{sl}$ for both orientations (τ_{cr}^{sl} are equal to 288 and 408 MPa at 20 and 60% strain, respectively, for [$\bar{1}$11]- and [$\bar{1}$44]-oriented crystals according to relation (5)). Consequently, there should be a change in the deformation mechanism from slip to twinning [59], which was found experimentally.

Thus, the estimated τ_{cr}^{tw} values, using relations (4), (6), and (7), show that the change in the deformation mechanism from slip to twinning in the CoCrFeNiMo$_{0.2}$ HEA single crystals occurs under the condition that the stresses are sufficient for breakaway a partial dislocation at γ_{ef} tending to zero, and when the condition $\tau_{cr}^{tw} \leq \tau_{cr}^{sl}$ is satisfied.

In the [001]-oriented CoCrFeNiMo$_{0.2}$ HEA crystals under tension, twinning by the mechanism of nucleation and growth of intrinsic SFs did not occur. In [001]-oriented crystals under tension, $m_1 < m_2$ and the factor Q = 0.12 changes its sign to the opposite in comparison with [$\bar{1}$11]- and [$\bar{1}$44]-oriented crystals [58,59]. This means that external stresses act on the first dislocation b_1 less than on the second b_2. According to relation (3), in [001]-oriented crystals under tension, γ_{ef} increases in the external stress field relative to γ_0, while the value of dislocation splitting, on the contrary, decreases. Indeed, in [001]-oriented crystals, according to relation (3), γ_{ef} increases to 0.036 and 0.04 J/m^2 relative to the equilibrium $\gamma_0 = 0.027$ J/m^2, respectively, with an increase in strain from 5 to 20%. The value of dislocation splitting, on the contrary, decreases to 2.1 and 1.9 nm, respectively, at 5–20% strain relative to the equilibrium dislocation splitting $d_0 = 2.8$ nm, which corresponds to $\gamma_0 = 0.027$ J/m^2. The condition for twinning is not reached, and in [001]-oriented CoCrFeNiMo$_{0.2}$ HEA crystals under tension, deformation develops only by slip at 77 K, as well as at 296 K.

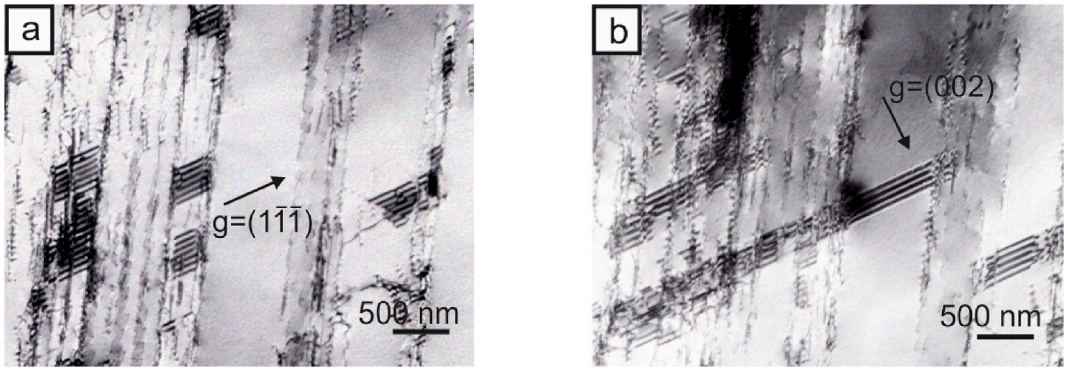

Fig. 10. TEM images showing stacking faults avalanche formation of in [$\bar{1}$11]-oriented single crystals of the CoCrFeNiMo$_{0.2}$ high-entropy alloy after tensile strain of 20% at 77 K.

The experimental values for τ_{cr}^{tw} in [$\bar{1}$11]- and [$\bar{1}$44]-oriented CoCrFeNiMo$_{0.2}$ HEA crystals and, for comparison, τ_{cr}^{tw} in HEAs and MEAs single and polycrystals with different γ_0 values, obtained from TEM, X-ray and DIC data [8,9,26,28–30,37,54,56], are presented in Table 2. Fig. 11 shows the dependence of τ_{cr}^{tw}/G(T) on γ_0/G(T)b$_1$ for [$\bar{1}$11]- and [$\bar{1}$44]-oriented single and polycrystals of HEAs and MEAs and single crystals of pure metals Ag and Cu obtained in Refs. [26,28,66]. An analysis of the presented data shows that, in the CoCrFeNiMo$_{0.2}$ HEA single crystals, τ_{cr}^{tw} and τ_{cr}^{tw} /G(T) determined by the TEM method depend on the crystal orientation at 77 K. The orientation dependence of τ_{cr}^{tw} is explained by the orientation dependence of γ_{ef} and strain hardening to twinning, according to relations (3 and 4). In [$\bar{1}$11]-oriented crystals at the same strain level, due to the difference in the Q factor, the nucleation of twins requires a higher stress level σ or a low value of γ_{ef} than in [$\bar{1}$44]-oriented crystals. Thus, in [$\bar{1}$11]-oriented crystals, the first isolated SFs appear at stress of 800 MPa, which is twice as high as σ = 400 MPa for the appearance of isolated SFs in [$\bar{1}$44]-oriented crystals.

The obtained experimental data of τ_{cr}^{tw} in the HEA single crystals with different γ_0 values show that the dependence of τ_{cr}^{tw}/G(T) on γ_0/G(T)b$_1$ in the HEA single crystals has the characteristic dependence for twinning in fcc pure metals and their substitutional alloys, namely, with an increase in γ_0 the τ_{cr}^{tw} increase (Fig. 11) [66]. The τ_{cr}^{sl} for slip in CoCrFeMnNi, CoCrFeNiAl$_{0.3}$, CoCrFeNiMo$_{0.2}$ and etc. HEAs turned out to be close (Table 1) [8,9]. At close τ_{cr}^{sl} values in the CoCrFeNiMo$_{0.2}$ HEA single crystals with γ_0 = 0.027 J/m^2, τ_{cr}^{tw} are higher than τ_{cr}^{tw} in the CoCrFeMnNi HEA single crystals with γ_0 = 0.018–0.022 J/m^2 and Fe40Mn40Co10Cr10HEA single crystals with γ_0 = 0.013 J/m^2 [54], but less than in the CoCrFeNiAl$_{0.3}$ HEA with γ_0 = 0.051 J/m^2 [8]. Therefore, the γ_0 value is an important parameter that determines twinning in fcc HEAs, as well as in fcc pure metals and their substitutional alloys [26–28,66]. On the other hand, in the CoCrFeNiMo$_{0.2}$ HEA single crystals with γ_0 = 0.027 J/m^2 close to γ_0 = 0.03 J/m^2 in Ag crystals, τ_{cr}^{tw} are 1.6–1.8 times higher at 77 K than for Ag crystals (Table 2). This is due, firstly, to the strong temperature dependence of τ_{cr}^{sl} (T) during solid-solution hardening with Mo atoms and, secondly, to the SRO influence on the development of twinning [9,44,45]. In crystals of pure Ag, the temperature dependence τ_{cr}^{sl} (T) is weak and there is no SRO [26,50,51].

In the [$\bar{1}$11]- and [$\bar{1}$44]-oriented CoCrFeNiMo$_{0.2}$ HEA crystals, τ_{cr}^{tw} for

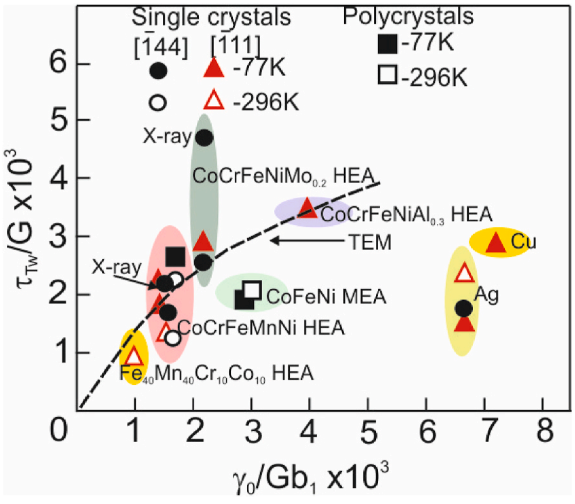

Fig. 11. Variation of the critical resolved shear stress for twinning normalized to shear modulus G, with the intrinsic stacking fault energy γ_0 normalized to Gb$_1$ (b$_1$ is Burgers vector of partial Shockley dislocation) in single and polycrystals of fcc medium- and high-entropy alloys and also in single crystals of fcc pure metals.

macrotwinning was 1.9 times higher than τ_{cr}^{tw} for the formation of isolated SFs and nanotwins, in contrast to Ag crystals with a similar γ_0, where the stresses for nucleation and propagation twins were close and there was no separation into nano- and macrotwinning [26–28]. Macrotwinning in the CoCrFeNiMo$_{0.2}$ HEA single crystals with γ_0 = 0.027 J/m^2 requires a high stress level compared to nanotwinning, as well as fulfillment of the condition $\tau_{cr}^{tw} < \tau_{cr}^{sl}$. In [$\bar{1}$44]-oriented crystals, macrotwinning developed, as in low-strength Ag crystals [26,28], after strain of 60% at the moment when the crystal axis reached the [001]- [$\bar{1}$11] boundary of the stereographic triangle due to dislocation slip (Fig. 6b), and in [$\bar{1}$11]-oriented crystals after 20% strain when twins were detected metallographically on the surface of the deformed specimen (Fig. 4g). As the value of γ_0 decreases, the difference in τ_{cr}^{tw} for nano- and macrotwinning should decrease. Previously, this was established for single crystals of the equiatomic CoCrFeMnNi HEA, in which γ_0 was 1.4 times less than in CoCrFeNiMo$_{0.2}$ HEA (Table 2) [9].

The dependence of the appearance of isolated SFs, large SFs and nanotwins and macrotwins on the stress level and crystal orientation is shown in Fig. 12. For comparison, data are also presented for single crystals and polycrystals of the equiatomic CoCrFeMnNi HEA [6,9,37]. It can be seen that, in the [$\bar{1}$44]-oriented CoCrFeNiMo$_{0.2}$ HEA crystals with the maximum factor Q, isolated SFs appear at a lower level of external stresses than in [$\bar{1}$11]-oriented crystals. But the stresses for large SFs and nanotwins are in the same stress range from 400 to 800 MPa for both [$\bar{1}$11] and [$\bar{1}$44] orientations. However, in [$\bar{1}$44]-oriented CoCrFeNiMo$_{0.2}$ HEA crystals, this stress level is reached at a higher slip strain than in [$\bar{1}$11]-crystals oriented for multiple slip or twinning. In this stress range, nanotwins also develop in single- and polycrystals of the equiatomic CoCrFeMnNi HEA [9,37]. The development of macrotwinning requires higher stresses of the order of 1000 MPa and above. A decrease in γ_0 shifts the transition of the macrotwinning deformation towards lower stresses, which was found in [$\bar{1}$44]-, [011]- and [$\bar{1}$23]- single crystals of the equiatomic CoCrFeMnNi HEA under tensile strain [9].

In polycrystalline HEAs, deformation by macrotwinning was not observed. This is due to several factors. Firstly, it is due to the absence of

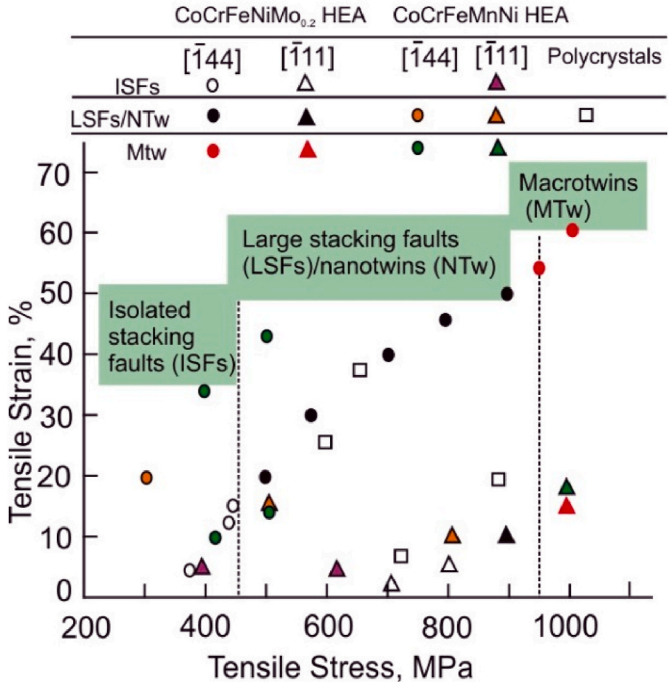

Fig. 12. Stacking faults, nanotwinning and macrotwinning as a function of stress in single crystals of the CoCrFeNiMo$_{0.2}$ HEA and in single and polycrystals of the equiatomic CoCrFeNiMn HEA under tensile strain.

a texture favorable for twinning. Most of the studies of the mechanical properties of fcc HEAs have been carried out on non-textured polycrystals [6,7]. Secondly, it is related to the small grain size. Twinning deformation was studied on fcc HEA polycrystals with grain size of 17–30 μm [7,37]. The nucleation of twins requires a significant local stress concentration, the sources of which are dislocation pile-ups near the grain boundaries. In crystals with a large grain size, more powerful dislocation pile-ups were observed than in polycrystals with a small grain size. As a result, in the case of a large grain, twinning developed easily in a wide temperature range [67]. Thirdly, the grain boundaries themselves in polycrystals are obstacles that limit the growth of twins in length [6,37,67].

Thus, the change in the deformation mechanism from slip to macrotwinning in the fcc HEAs is determined by the γ_0 value, the crystal orientation, or, for polycrystals, by the texture and grain size.

4.2. Twinning-induced plasticity in $CoCrFeNiMo_{0.2}$ HEA single crystals

Studies of the mechanical behavior of the $CoCrFeNiMo_{0.2}$ HEA single crystals shows that they demonstrate an exceptional combination of strength and plasticity at 77 K, which is characteristic of TWIP steels (Figs. 3 and 5) [12,31]. The increase in plasticity at 77 K in [$\bar{1}$11]-oriented crystals and especially in [$\bar{1}$44]-oriented crystals is due to several factors. Firstly, the combination of a high stress level at the yield point at 77 K ($\sigma_{0.1}$(77 K) = 430–650 MPa) due to solid solution hardening by Mo atoms with γ_0 = 0.027 J/m^2 leads to the development of a planar dislocation structure with dislocation pile-ups and multipoles and localization of slip deformation predominantly in one system [8,9]. Secondly, the combination of a high stress level due to solid solution hardening by Mo atoms with γ_0 = 0.027 J/m^2 leads to the development of macrotwinning mainly in one system after a significant strain level of slip deformation and to the manifestation of the TWIP-effect, as in single crystals of the equiatomic CoCrFeMnNi HEA [9,12,31]. Thirdly, Θ_{II} remains high during plastic deformation due to the development of nanotwinning simultaneously with slip. All this in combination complicates the processes of neck formation, which requires the development of slip simultaneously in several systems, complicates the processes of dynamic recovery and shifts the Considère condition for neck formation to the region of large deformations [9,12,31]:

$$\sigma \geq \frac{d\sigma}{d\varepsilon}, \tag{8}$$

here, σ is the tensile stress, ε is the tensile strain. For example, in [$\bar{1}$44]-oriented crystals at 77 K, with the development of deformation first by nanotwinning simultaneously with slip, and then transition to deformation by macrotwinning in one system, the plasticity reached 106%. At 77 K in these crystals, condition (8) for the neck formation was achieved at σ = 1440 MPa, which was significantly higher than the stresses for neck formation at 296 K, when the deformation developed only by slip (Fig. 5). As for [$\bar{1}$11]-oriented crystals, the plasticity increased by 7% at 77 K relative to 296 K. In [$\bar{1}$11]-oriented crystals at 77 K, condition (8) for the neck formation was achieved at σ = 1680 MPa, which was also significantly higher than the stresses for neck formation at 296 K, when the deformation developed by slip (Fig. 3). In [001]-oriented crystals, with the development of deformation only by slip, plasticity was close at both temperatures (77 and 296 K) (Fig. 8). Slip developed in several systems from the beginning of plastic deformation, and condition (8) for the neck formation was achieved at strain that was significantly less than in [$\bar{1}$11]- and [$\bar{1}$44]-oriented crystals during the development of deformation by slip and twinning. In [001]-oriented crystals, the stresses σ = 990 MPa for the neck formation at 77 K were 380 MPa higher than these stresses at 296 K, which was due to the strong temperature dependence $\sigma_{0.1}$(T). At 296 and 77 K, the difference between the stresses at the yield point and the stresses for neck formation was close in the case of [001]-oriented crystals under slip deformation, but notable differed in the case of [$\bar{1}$11]- and [$\bar{1}$44]-oriented crystals, when twinning developed with slip (Figs. 3 and 5).

Previously, similar results on the effect of twinning on plasticity were obtained on single crystals of the equiatomic CoCrFeMnNi HEA [9]. For example, in the [$\bar{1}$23]-oriented CoCrFeMnNi HEA crystals at 77 K, with the development of twinning in one system after previous slip deformation, the plasticity reached 117% and was twice as high as the plasticity at 296 K in the case of slip deformation in crystals of this orientation. With multiple twinning, which developed practically at the beginning of plastic deformation in the [$\bar{1}$44]-oriented CoCrFeMnNi HEA crystals at 77 K, plasticity decreased up to 50% [9]. In the [$\bar{1}$44]-oriented $CoCrFeNiMo_{0.2}$ crystals, as a result of an increase in γ_0, enhancement of the SRO and localization of deformation predominantly in one system upon alloying with Mo atoms, macrotwinning developed predominantly in one system simultaneously with slip at 77 K. This shifted the stresses for neck formation according to condition (8) to the high strain levels, as in the [$\bar{1}$11]-, [$\bar{1}$23]- and [011]-oriented CoCrFeMnNi HEA crystals [9].

An analysis of the results obtained on the $CoCrFeNiMo_{0.2}$ HEA single crystals in the present paper and on the equiatomic CoCrFeMnNi HEA single crystals in Ref. [9], revealed general regularities in the effect of twinning on plasticity and on the TWIP-effect in fcc HEAs. It was shown that by controlling the number of active twinning systems by choosing the crystal orientation, one can control the plasticity and the TWIP-effect. Thus, experiments using single crystals provide valuable information on the development of twinning and its effect on hardening and plasticity, which is necessary for analysis the mechanical behavior of textured polycrystals of HEAs. Thus, $CoCrFeNiMo_{0.2}$ HEA obtained by laser melting was characterized by a sharp <001> texture [46]. In this case, the shape of the flow curves, strain hardening coefficient and plasticity turned out to be close to the mechanical behavior of [001]-oriented crystals, in which deformation was realized only by slip.

5. Summary and conclusions

The mechanical behavior and mechanisms of deformation (slip and twinning) of the $CoCrFeNiMo_{0.2}$ HEA single crystals under tensile strain were studied, which revealed the following regularities at 296 and 77 K.

1. Single crystals of the $Co_{24}Cr_{24}Fe_{24}Ni_{24}Mo_4$ (at.%) HEA with a stacking fault energy of γ_0 = 0.027 J/m^2 were obtained, when alloying an equiatomic CoCrFeNi HEA with Mo atoms up to 4 at.% by reducing each element in equal atomic percentages.
2. It was shown that alloying with Mo atoms up to 4 at.% leads to solid solution hardening, at which the CRSS for slip τ_{cr}^{sl} in the $CoCrFeNiMo_{0.2}$ HEA single crystals exceeded τ_{cr}^{sl} in the equiatomic CoCrFeMnNi HEA single crystals. At temperatures of 77 and 296 K, the CRSS for slip in the single crystals of the CoCrFeNiMo0.2 HEA do not depend on the crystal orientation under tensile and the Schmid law is satisfied. Fulfillment of the Schmid law for the CRSS at slip is a general regularity in the stable fcc HEAs with stacking fault energy of γ_0 = 0.019–0.051 J/m^2.
3. It was established that in the [$\bar{1}$11]- and [$\bar{1}$44]-oriented $CoCrFeNiMo_{0.2}$ HEA crystals, with γ_0 = 0.027 J/m^2, twinning develops under tensile strain at 77 K, while at 296 K it is not observed. In [001]-oriented crystals of this alloy, twinning is not found at 296 and 77 K. Two types of twins are found in the [$\bar{1}$11]- and [$\bar{1}$44]-oriented crystals. The first type is nanotwinning with a thickness of 5–10 nm, which develops in the [$\bar{1}$11]- and [$\bar{1}$44]-oriented crystals after low strain level ε ≥ 5% simultaneously with slip and is detected only by TEM in the study of the dislocation structure. The nanotwins-slip interaction leads to a sharp increase in the strain hardening coefficient Θ = dσ/dε and the appearance of the TWIP-effect. The second type is macrotwinning (thickness 100–600 nm), which develops after strain of 20 and 60% at 77 K, respectively, in the [$\bar{1}$11]- and

[$\bar{1}44$]-oriented crystals. In [$\bar{1}11$]-oriented crystals, macrotwinning is determined metallographically on the surface of deformed crystals. In [$\bar{1}44$]-oriented crystals, macrotwinning is detected both optical and X-ray studies on the surface of deformed crystals and at the precession of the crystal axis. In [$\bar{1}44$]-oriented crystals, macrotwins appears on the surface of deformed crystals at strain of 60%, when the crystal axis changes its direction from slip [$\bar{1}01$] to twinning [$\bar{2}11$] with increasing tensile strain. Macrotwinning develops predominantly in the primary twinning system [$\bar{2}11$] (111) and its development is accompanied by a decrease in $\Theta = d\sigma/d\varepsilon$, especially in [$\bar{1}44$]-oriented crystals. In [$\bar{1}44$]-oriented crystals during the development of nanotwins with slip $\Theta = 2000$ MPa, which decreased to $\Theta = 950$–1050 MPa when macrotwinning develops predominantly in one system.

4. The τ_{cr}^{tw} for nano- and macrotwins depend on the crystal orientation. For nanotwinning, $\tau_{cr}^{tw} = 212$ MPa in [$\bar{1}44$]-oriented crystals and $\tau_{cr}^{tw} = 250$ MPa in [$\bar{1}11$]-oriented crystals. The CRSS for macrotwinning are 1.3 and 1.9 higher than for nanotwinning, respectively, for [$\bar{1}11$]- and [$\bar{1}44$]-oriented crystals. τ_{cr}^{tw} for macrotwinning is 400 MPa in [$\bar{1}44$]-oriented crystals, and 335 MPa in [$\bar{1}11$]-oriented crystals. For the transition to deformation by macrotwinning, it is necessary that the value of the effective stacking fault energy γ_{ef} tend to zero and the condition $\tau_{cr}^{tw} < \tau_{cr}^{sl}$ was achieved.
5. It has been established that in the [$\bar{1}44$]-oriented $CoCrFeNiMo_{0.2}$ HEA crystals, the development of macrotwinning predominantly in one system at 77 K suppresses slip multiplicity and shifts neck formation according to the Considère condition to high strain levels and increases plasticity of crystals by a factor of 1.5 compared to the room temperature. In [$\bar{1}44$]-oriented crystals, plasticity is 70% under slip deformation at 296 K, and it increased up to 106% at 77 K, when macrotwinning develops predominantly in one system. In [001]-oriented crystals, upon only slip deformation, plasticity is 35–37% and does not depend on the test temperature.

Funding

This study was supported by the Tomsk State University Development Programme (Priority-2030). Work was conducted with the application of equipment of the Tomsk Regional Core Shared Research Facilities Centre of National Research Tomsk State University.

CRediT authorship contribution statement

I.V. Kireeva: Supervision, Conceptualization, Investigation, Writing – original draft, Writing – review & editing, Project administration, Funding acquisition. **Yu.I. Chumlyakov:** Conceptualization, Supervision. **A.V. Vyrodova:** Investigation. **A.A. Saraeva:** Investigation.

Declaration of competing interest

The authors declare that they have no known competing financial interests or personal relationships that could have appeared to influence the work reported in this paper.

Data availability

Data will be made available on request.

References

[1] B. Cantor, I.T.H. Chang, P. Knight, A.J.B. Vincent, Microstructural development in equiatomic multicomponent alloys, Mater. Sci. Eng., A 375-377 (2004) 213–218, https://doi.org/10.1016/j.msea.2003.10.257.
[2] Y. Zhang, T.T. Zuo, Z. Tang, M.C. Gao, K.A. Dahmen, P.K. Liaw, Z.P. Lu, Microstructures and properties of high-entropy alloys, Prog. Mater. Sci. 61 (2014) 1–93, https://doi.org/10.1016/j.pmatsci.2013.10.001.
[3] A.J. Zaddach, C. Niu, C.C. Koch, D.L. Irving, Mechanical properties and stacking fault energies of NiFeCrCoMn high-entropy alloy, JOM 65 (12) (2013) 1780–1789, https://doi.org/10.1007/s11837-013-0771-4.
[4] Z. Wu, H. Bei, G.M. Pharr, E.P. George, Temperature dependence of the mechanical properties of equiatomic solid solution alloys with face-centered cubic crystal structures, Acta Mater. 81 (2014) 428–441, https://doi.org/10.1016/j.actamat.2014.08.026.
[5] P. Wilson, R. Field, M. Kaufman, The use of diffusion multiples to examine the compositional dependence of phase stability and hardness of the Co-Cr-Fe-Mn-Ni high entropy alloy system, Intermetallics 75 (2016) 15–24, https://doi.org/10.1016/j.intermet.2016.04.007.
[6] F. Otto, A. Dlouhy, Ch. Somsen, H. Bei, G. Eggeler, E.P. George, The influences of temperature and microstructure on the tensile properties of a CoCrFeMnNi high-entropy alloy, Acta Mater. 61 (15) (2013) 5743–5755, https://doi.org/10.1016/j.actamat.2013.06.018.
[7] S.-H. Joo, H. Kato, M.J. Jang, J. Moon, C.W. Tsai, J.W. Yeh, H.S. Kim, Tensile deformation behavior and deformation twinning of an equimolar CoCrFeMnNi high-entropy alloy, Mater. Sci. Eng., A 689 (2017) 122–133, https://doi.org/10.1016/j.msea.2017.02.043.
[8] I.V. Kireeva, Yu.I. Chumlyakov, Z.V. Pobedennaya, A.V. Vyrodova, I. V. Kuksgauzen, D.A. Kuksgauzen, Orientation and temperature dependence of a planar slip and twinning in single crystals of $Al_{0.3}CoCrFeNi$ high-entropy alloy, Mater. Sci. Eng., A 737 (2018) 47–60, https://doi.org/10.1016/j.msea.2018.09.025.
[9] I.V. Kireeva, Yu.I. Chumlyakov, A.V. Vyrodova, Z.V. Pobedennaya, I. Karaman, Effect of twinning on the orientation dependence of mechanical behaviour and fracture in single crystals of the equiatomic CoCrFeMnNi high-entropy alloy at 77K, Mater. Sci. Eng., A 784 (1–14) (2020), 139315, https://doi.org/10.1016/j.msea.2020.139315.
[10] W. Li, P.K. Liaw, Y. Gao, Fracture resistance of high entropy alloys: a review, Intermetallics 99 (2018) 69–83, https://doi.org/10.1016/j.intermet.2018.05.013.
[11] B. Gludovatz, A. Hohenwarter, D. Catoor, E.H. Chang, E.P. George, R.O. Ritchie, A fracture-resistant high-entropy alloy for cryogenic applications, Science 345 (6201) (2014) 1153–1158, https://doi.org/10.1126/science.1254581.
[12] B.C. De Cooman, Yu. Estrin, S.K. Kim, Twinning-induced plasticity (TWIP) steels, Acta Mater. 142 (2018) 283–362, https://doi.org/10.1016/j.actamat.2017.06.046.
[13] Y.Y. Zhao, H.W. Chen, Z.P. Lu, T.G. Nieh, Thermal stability and coarsening of coherent particles in a precipitation-hardened $(NiCoFeCr)_{94}Ti_2Al_4$ high-entropy alloy, Acta Mater. 147 (2018) 184–194, https://doi.org/10.1016/actamat.2018.01.049.
[14] H.Y. Yasuda, H. Miyamoto, K. Cho, T. Nagase, Formation of ultrafine-grained microstructure in $Al_{0.3}CoCrFeNi$ high entropy alloys with grain boundary precipitates, Mater. Lett. 199 (2017) 120–123, https://doi.org/10.1016/j.matlet.2017.04.072.
[15] D. Li, C. Li, T. Feng, Y. Zhang, G. Sha, J.J. Lewandowski, P.K. Liaw, Y. Zhang, High-entropy $Al_{0.3}CoCrFeNi$ alloy fibers with high tensile strength and ductility at ambient and cryogenic temperatures, Acta Mater. 123 (2017) 285–294, https://doi.org/10.1016/j.actamat.2016.10.038.
[16] J.Y. He, H. Wang, H.L. Huang, X.D. Xu, M.W. Chen, Y. Wu, X.J. Liu, T.G. Nieh, K. An, Z.P. Lu, A precipitation-hardened high-entropy alloy with outstanding tensile properties, Acta Mater. 102 (2016) 187–196, https://doi.org/10.1016/actamat.2015.08.076.
[17] W.H. Liu, Z.P. Lu, J.Y. He, J.H. Luan, Z.J. Wang, B. Liu, Y. Liu, M.W. Chen, C.T. Liu, Ductile CoCrFeNiMox high entropy alloys strengthened by hard intermetallic phases, Acta Mater. 116 (2016) 332–342, https://doi.org/10.1016/j.actamat.2016.06.063.
[18] E.G. Astafurova, K.A. Reunova, E.V. Melnikov, M.Yu. Panchenko, S.V. Astafurov, G.G. Maier, V.A. Moskvina, On the difference in carbon- and nitrogen-alloying of equiatomic FeMnCrNiCo high-entropy alloy, Mater. Lett. 276 (1–4) (2020), 128183, https://doi.org/10.1016/j.matlet.2020.128183.
[19] I.V. Kireeva, Yu.I. Chumlyakov, A.A. Saraeva, A.V. Vyrodova, Z.V. Pobedennaya, I. V. Kuksgauzen, D.A. Kuksgauzen, Mechanical behavior of differently oriented $(CoCrFeNi)_{94}Ti_2Al_4$ single crystals, Phys. Mesomech. 24 (6) (2021) 633–641, https://doi.org/10.1134/S1029959921060011.
[20] I.V. Kireeva, A.A. Saraeva, A.V. Vyrodova, Yu.I. Chumlyakov, Orientation dependence of the mechanical behaviour of $(CoCrFeNi)_{94}Ti_2Al_4$ high-entropy alloy single crystals with γ'-phase particles, Mater. Lett. 305 (1–4) (2021), 130746, https://doi.org/10.1016/j.matlet.2021.130746.
[21] I.V. Kireeva, Yu.I. Chumlyakov, Z.V. Pobedennaya, A.V. Vyrodova, Effect of γ'-phase particles on the orientation and temperature dependence of the mechanical behaviour of $Al_{0.3}CoCrFeNi$ high entropy alloy single crystals, Mater. Sci. Eng., A 772 (1–9) (2020), 138772, https://doi.org/10.1016/j.msea.2019.138772.
[22] T.T. Shun, L.Y. Chang, M.H. Shiu, Microstructure and mechanical properties of multiprincipal component $CoCrFeNiMo_x$ alloys, Mater. Char. 70 (2012) 63–67, https://doi.org/10.1016/j.matchar.2012.05.005.
[23] F. Xiong, R. Fu, Y. Li, B. Xu, X. Qi, Influences of nitrogen alloying on microstructural evolution and tensile properties of CoCrFeMnNi high-entropy alloy treated by cold-rolling and subsequent annealing, Mater. Sci. Eng., A 787 (1–11) (2020), 139472, https://doi.org/10.1016/j.msea.2020.139472.
[24] I.V. Kireeva, Yu.I. Chumlyakov, Z.V. Pobedennaya, A.V. Vyrodova, A.A. Saraeva, High-strength behavior of the $Al_{0.3}CoCrFeNi$ high-entropy alloy single crystals, Metals 10 (9) (2020) 1149, https://doi.org/10.3390/met10091149, 1-11.

[25] S. Dasari, A. Sarkar, A. Sharma, B. Gwalani, D. Choudhuri, V. Soni, S. Manda, I. Samajdar, R. Banerjee, Recovery of cold-worked $Al_{0.3}$CoCrFeNi complex concentrated alloy through twinning assisted B2 precipitation, Acta Mater. 202 (2021) 448–462, https://doi.org/10.1016/j.actamat.2020.10.071.
[26] J.W. Christian, S. Mahajan, Deformation twinning, Prog. Mater. Sci. 39 (1–2) (1995) 1–157, https://doi.org/10.1016/0079-6425(94)00007-7.
[27] N. Narita, J. Takamura, Deformation twinning in silver-and copper-alloy crystals, Philos. Mag. 29 (5) (1974) 1001–1028, https://doi.org/10.1080/14786437408226586.
[28] N. Narita, J.-I. Takamura, Deformation twinning in fcc and bcc metals, Dislocation Solid. 9 (1992) 135–189.
[29] M. Bönisch, Y. Wu, H. Sehitoglu, Hardening by slip-twin and twin-twin interactions in FeMnNiCoCr, Acta Mater. 153 (2018) 391–403, https://doi.org/10.1016/j.actamat.2018.04.054.
[30] W. Abuzaid, H. Sehitoglu, Critical resolved shear stress for slip and twin nucleation in single crystalline FeNiCoCrMn high entropy alloy, Mater. Char. 129 (2017) 288–299, https://doi.org/10.1016/j.matchar.2017.05.014.
[31] P. Chowdhury, D. Canadinc, H. Sehitoglu, On deformation behavior of Fe-Mn based structural alloys, Mater. Sci. Eng. R 122 (2017) 1–28, https://doi.org/10.1016/j.mser.2017.09.002.
[32] I.V. Kireeva, Yu.I. Chumlyakov, Effect of nitrogen and stacking -fault energy on twinning in [111] single crystals of austenitic stainless steels, Phys. Met. Metallogr. 108 (3) (2009) 298–309, https://doi.org/10.1134/S0031918X09090117.
[33] I.V. Kireeva, Yu.I. Chumlyakov, Z.V. Pobedennaya, A.V. Vyrodova, I. Karaman, Twinning in [001]-oriented single crystals of CoCrFeMnNi high-entropy alloy at tensile deformation, Mater. Sci. Eng., A 713 (2018) 253–259, https://doi.org/10.1016/j.msea.2017.12.059.
[34] I. Karaman, H. Sehitoglu, Y.I. Chumlyakov, H.J. Maier, The deformation of low-stacking fault-energy austenitic steels, JOM 54 (7) (2002) 31–37, https://doi.org/10.1007/BF02700983.
[35] S.W. Wu, G. Wang, J. Yi, Y.D. Jia, I. Hussain, Q.J. Zhai, P.K. Liaw, Strong grain-size effect on deformation twinning of an $Al_{0.1}$CoCrFeNi high-entropy alloy, Mater. Res. Lett. 5 (4) (2017) 276–283, https://doi.org/10.1080/21663831.2016.1257514.
[36] J. Joseph, N. Stanford, P. Hodgson, D.M. Fabijanic, Tension/compression asymmetry in additive manufactured face centered cubic high entropy alloy, Scripta Mater. 129 (2017) 30–34, https://doi.org/10.1016/j.scriptamat.2016.10.023.
[37] G. Laplanche, A. Kostka, O.M. Horst, G. Eggeler, E.P. George, Microstructure evolution and critical stress for twinning in the CrMnFeCoNi high-entropy alloy, Acta Mater. 118 (2016) 152–163, https://doi.org/10.1016/j.actamat.2016.07.038.
[38] E.G. Astafurova, I.V. Kireeva, Yu.I. Chumlyakov, H.J. Maier, H. Sehitoglu, The influence of orientation and aluminium content on the deformation mechanisms of Hadfield steel single crystals, Int. J. Mater. Res. 98 (2) (2007) 144–149, https://doi.org/10.3139/146.101438.
[39] F. Pettinari, J. Douin, G. Saada, P. Caron, A. Coujou, N. Clément, Stacking fault energy in short-range ordered γ-phases of Ni-based superalloys, Mater. Sci. Eng., A 325 (1–2) (2002) 511–519, https://doi.org/10.1016/S0921-5093(01)01765-8.
[40] F. Pettinari-Sturnel, A. Coujou, N. Clement, The fluctuation of short-range order evidenced by mobile dislocations in the γ-phase of a nickel-based superalloy, Mater. Sci. Eng., A 400-401 (2005) 114–117, https://doi.org/10.1016/j.msea.2005.02.072.
[41] J. Miao, C. Slone, S. Dasari, M. Ghazisaeidi, R. Banerjee, E.P. George, M.J. Mills, Ordering effects on deformation substructures and strain hardening behavior of a CrCoNi based medium entropy alloy, Acta Mater. 210 (1–20) (2021), 116829, https://doi.org/10.1016/j.actamat.2021.116829.
[42] I.V. Kireeva, Yu.I. Chumlyakov, N.V. Luzginova, Slip and twinning in single crystals of austenitic stainless steels with nitrogen, Phys. Met. Metallogr. 94 (5) (2002) 508–519.
[43] V. Gerold, H.P. Karnthaler, On the origin of planar slip in F.C.C. alloys, Acta Metall. 37 (8) (1989) 2177–2183, https://doi.org/10.1016/0001-6160(89)90143-0.
[44] J.B. Cohen, M.E. Fine, Some aspects of short-range order, J. Phys. Radium 23 (10) (1962) 749–762, https://doi.org/10.1051/jphysrad:019620023010074901.
[45] J.A. Venables, The electron microscopy of deformation twinning, J. Phys. Chem. Solid. 25 (7) (1964) 685–690, https://doi.org/10.1016/0022-3697(64)90177-5.
[46] Q. Wang, A. Amar, C. Jiang, H. Luan, S. Zhao, H. Zhang, G. Le, X. Liu, X. Wang, X. Yang, J. Li, CoCrFeNiMo$_{0.2}$ high entropy alloy by laser melting deposition: prospective material for low temperature and corrosion resistant applications, Intermetallics 119 (1–6) (2020), 106727, https://doi.org/10.1016/j.intermet.2020.106727.
[47] T.T. Shun, L.Y. Chang, M.H. Shiu, Age-hardening of the CoCrFeNiMo$_{0.85}$ high entropy alloy, Mater. Char. 81 (2013) 92–96, https://doi.org/10.1016/j.matchar.2013.04.012.
[48] B. Cai, B. Liu, S. Karba, Y. Wang, K. Yan, P.D. Lee, Y. Liu, Deformation mechanisms of Mo alloyed FeCoCrNi high entropy alloy: in situ neutron diffraction, Acta Mater. 127 (2017) 471–480, https://doi.org/10.1016/j.actamat.2017.01.034.
[49] C.S. Barrett, T.B. Massalski, Structure of Metals: Crystallographic Methods, Principles, and Data, Pergamon, New York, NY, 1980.
[50] R.W.K. Honeycombe, The Plastic Deformation of Metals, Arnold, London, 1968 translated under the title Plasticheskya deformatsiya metallov, Moscow: Mir Publ.; 1972. (In Russian).
[51] R. Berner, H. Kronmuller, Plasticheskya deformatsiya monokristallov [Plastische Verformung von Eikristallen], Mir Publ., Moscow, 1969 (In Russian).
[52] I.V. Kireeva, Yu.I. Chumlyakov, Z.V. Pobedennaya, Yu.N. Platonova, I. V. Kuksgauzen, D.A. Kuksgauzen, V.V. Poklonov, I. Karaman, H. Sehitoglu, Slip and twinning in the [149] - oriented single crystals of a high-entropy alloy, Russ. Phys. J. 59 (8) (2016) 1242–1250, https://doi.org/10.1007/s11182-016-0898-1.
[53] I.V. Kireeva, Yu.I. Chumlyakov, Z.V. Pobedennaya, I.V. Kuksgauzen, I. Karaman, Orientation dependence of twinning in single crystalline CoCrFeMnNi high-entropy alloy, Mater. Sci. Eng., A 705 (2017) 176–181, https://doi.org/10.1016/j.msea.2017.08.065.
[54] S. Picak, J. Liu, C. Hayrettin, W. Nasim, D. Canadinc, K.Y. Xie, Y.I. Chumlyakov, I. V. Kireeva, I. Karaman, Anomalous work hardening behavior of $Fe_{40}Mn_{40}Cr_{10}Co_{10}$ high entropy alloy single crystals deformed by twinning and slip, Acta Mater. 181 (2019) 555–569, https://doi.org/10.1016/j.actamat.2019.09.048.
[55] D.D. Zhang, J.Y. Zhang, J. Kuang, G. Liu, J. Sun, Superior strength-ductility synergy and strain hardenability of Al/Ta co-doped NiCoCr twinned medium entropy alloy for cryogenic applications, Acta Mater. 220 (1–13) (2021), 117288, https://doi.org/10.1016/j.actamat.2021.117288.
[56] M. Schneider, G. Laplache, Effects of temperature on mechanical properties and deformation mechanisms of the equiatomic CrFeNi medium-entropy alloy, Acta Mater. 204 (1–16) (2021), 116470, https://doi.org/10.1016/j.actamat.2020.11.012.
[57] B. Uzer, S. Picak, J. Liu, T. Jozaghi, D. Canadinc, I. Karaman, Y.I. Chumlyakov, I. Kireeva, On the mechanical response and microstructure evolution of NiCoCr single crystalline medium entropy alloys, Mater. Res. Lett. 6 (8) (2018) 442–449, https://doi.org/10.1080/21663831.2018.1478331.
[58] S.M. Copley, B.H. Kear, The dependence of the width of a dissociated dislocation on dislocation velocity, Acta Metall. 16 (2) (1968) 227–231, https://doi.org/10.1016/0001-6160(68)90118-1.
[59] T.S. Byun, On the stress dependence of partial dislocation separation and deformation microstructure in austenitic stainless steel, Acta Mater. 51 (11) (2003) 3063–3071, https://doi.org/10.1016/S1359-6454(03)00117-4.
[60] Z. Zhang, M.M. Mao, J. Wang, B. Gludovatz, Z. Zhang, S.X. Mao, E.P. George, Q. Yu, R.O. Ritchie, Nanoscale origins of the damage tolerance of the high-entropy alloy CrMnFeCoNi, Nat. Commun. 6 (1–6) (2015), 10143, https://doi.org/10.1038/ncomms10143.
[61] T.M. Smith, M.S. Hooshmand, B.D. Esser, F. Otto, D.W. McComb, E.P. George, M. Ghazisaeidi, M.J. Mills, Atomic-scale characterization and modeling of 60° dislocation in a high-entropy alloy, Acta Mater. 110 (2016) 352–363, https://doi.org/10.1016/j.actamat.2016.03.045.
[62] J.P. Hirth, J. Lothe, Theory of Dislocations, McGraw-Hill, New York, 1968.
[63] C.X. Huang, K. Wang, S.D. Wu, Z.F. Zhang, G.Y. Li, S.X. Li, Deformation twinning in polycrystalline copper at room temperature and low strain rate, Acta Mater. 54 (3) (2006) 655–665, https://doi.org/10.1016/j.actamat.2005.10.002.
[64] G. Laplanche, P. Gadaud, O. Horst, F. Otto, G. Eggeler, E.P. George, Temperature dependencies of the elastic moduli and thermal expansion coefficient of an equiatomic single-phase CoCrFeMnNi high-entropy alloy, J. Alloys Compd. 623 (2015) 348–353, https://doi.org/10.1016/j.jallcom.2014.11.061.
[65] T.S. Byun, E.H. Lee, J.D. Hunn, Plastic deformation in 316LN stainless steel – characterization of deformation microstructures, J. Nucl. Mater. 321 (1) (2003) 29–39, https://doi.org/10.1016/S0022-3115(03)00195-8.
[66] L. Remy, The interaction between slip and twinning systems and the influence of twinning on the mechanical behavior of fcc materials and alloys, Metall. Trans. A 12 (3) (1981) 387–408, https://doi.org/10.1007/BF02648536.
[67] J.H. Kim, K.R. Lim, J.W. Won, Y.S. Na, H.S. Kim, Mechanical properties and deformation twinning behavior of as-cast CoCrFeMnNi high-entropy alloy at low and high temperatures, Mater. Sci. Eng., A 712 (2018) 108–113, https://doi.org/10.1016/j.msea.2017.11.081.